Konrad-Zuse-Zentrum
für Informationstechnik Berlin

Takustraße 7
D-14195 Berlin-Dahlem
Germany

SUSANNA RÖBLITZ, CLAUDIA STÖTZEL, PETER DEUFLHARD,
HANNAH M. JONES, DAVID-OLIVIER AZULAY, PIET VAN DER GRAAF,
STEVEN W. MARTIN

A mathematical model of the human menstrual cycle for the administration of GnRH analogues

ZIB-Report 11-16 (April 2011)

A mathematical model of the human menstrual cycle for the administration of GnRH analogues

Susanna Röblitz [*] Claudia Stötzel [*] Peter Deuflhard [*]
Hannah M. Jones [†] David-Olivier Azulay [‡] Piet van der Graaf [§]
Steven W. Martin [§]

April 28, 2011

Abstract

This study presents a differential equation model for the feedback mechanisms between Gonadotropin-releasing Hormone (GnRH), Follicle-Stimulating Hormone (FSH), Luteinizing Hormone (LH), development of follicles and corpus luteum, and the production of estradiol (E2), progesterone (P4), inhibin A (IhA), and inhibin B (IhB) during the female menstrual cycle. In contrast to other models, this model does not involve delay differential equations and is based on deterministic modelling of the GnRH pulse pattern, which allows for faster simulation times and efficient parameter identification. These steps were essential to tackle the task of developing a mathematical model for the administration of GnRH analogues. The focus of this paper is on model development for GnRH receptor binding and the integration of a pharmacokinetic/pharmacodynamic model for the GnRH agonist Nafarelin and the GnRH antagonist Cetrorelix into the menstrual cycle model. The final mathematical model describes the hormone profiles (LH, FSH, P4, E2) throughout the menstrual cycle in 12 healthy women. Moreover, it correctly predicts the changes in the cycle following single and multiple dose administration of Nafarelin or Cetrorelix at different stages in the cycle.

AMS MSC 2000: 92C42, 92C30, 90C31, 65L09

Keywords: human menstrual cycle, mathematical modelling, GnRH analogues, differential equations, systems biology

1 Introduction

The gonadotropin-releasing hormone (GnRH) plays an important role in the female reproductive cycle. GnRH controls the complex process of follicular growth, ovulation, and corpus luteum development. It is responsible for the synthesis and release of gonadotropins (follicle-stimulating hormone (FSH) and luteinizing hormone (LH)) from the anterior pituitary to the blood. These processes are controlled by the size and frequency of GnRH pulses. In males, the GnRH pulse frequency is constant, but in females, the frequency varies during the menstrual cycle, with a large surge of GnRH just before ovulation. Low-frequency pulses lead to FSH release, whereas high frequency pulses stimulate LH release. Thus, pulsatile GnRH secretion is necessary for correct reproductive function.

[*]Zuse Institute Berlin, Takustraße 7, D-14195 Berlin, Germany. Supported by DFG Research Center Matheon "Mathematics for Key Technologies", Berlin, Germany.
[†]Department of Pharmacokinetics, Dynamics and Metabolism, Pfizer, Ramsgate Road, Sandwich, Kent CT13 9NJ, United Kingdom.
[‡]Molecular Medicine, Pfizer, Ramsgate Road, Sandwich, Kent CT13 9NJ, United Kingdom.
[§]Department of Clinical Pharmacology, Pfizer, Ramsgate Road, Sandwich, Kent CT13 9NJ, United Kingdom.

Since GnRH itself is of limited clinical use due to its short half-life, modifications of its structure have led to GnRH analog medications that either stimulate (GnRH agonists) or suppress (GnRH antagonists) the gonadotropins. Agonists do not quickly dissociate from the GnRH receptor, resulting in an initial increase in FSH and LH secretion ("flare effect"). After their initial stimulating action, agonists are able to exert a prolonged suppression effect , termed "downregulation" or "desensitization", which can be observed after about 10 days. Generally this induced and reversible hypogonadism is the therapeutic goal. GnRH agonists are used, for example, for the treatment of cancer, endometriosis, uterine fibroids, and precocious puberty [10].

GnRH antagonists compete with natural GnRH for binding to GnRH receptors, thus leading to an acute suppression of the hypothalamic-pituitary-gonadal axis without an initial surge. For several reasons, such as high dosage requirements, the commercialization of GnRH antagonists lagged behind their agonist counterparts [12]. Today, GnRH antagonists are mainly used in IVF treatment to block natural ovulation (Cetrorelix, Ganorelix) and in the treatment of prostate cancer (Abarelix, Degarelix) [10].

The fundamental understanding of the receptor response is necessary to create safer pharmaceutical drugs. Therefore, the aim of this paper is to develop a mathematical model that characterizes the different actions of GnRH agonists and antagonists by their different effects on the GnRH receptor binding mechanisms. The model should be able to explain measurement values for the blood concentrations of LH, FSH, estradiol (E2), and progesterone (P4) after single and multiple dose treatment with a GnRH agonist or antagonist. Such a model should eventually help in preparing and monitoring clinical trials with new drugs that affect GnRH receptors.

There are only a few publications available that focus on feedback mechanisms in the female menstrual cycle. In 1999, a differential equation model that contains the regulation of LH and FSH synthesis, release, and clearance by E2, P4, and inhibin was introduced by Schlosser and Selgrade [36, 33]. This model was extended by Selgrade [35], Harris [16, 17] and later by Pasteur [30] to describe the roles of LH and FSH during the development of ovarian follicles and the production of the ovarian hormones E2, P4, inhibin A (IhA), and inhibin B (IhB). Reinecke and Deuflhard [32, 31] added, among other things, a stochastic GnRH pulse generator and GnRH receptor binding mechanisms. This model was insufficient for our purpose and needed modifications.

On the other hand, there exist pharmacokinetic/pharmacodynamic (PK/PD) models for GnRH analogues [28, 38, 20]. These models describe the influence on LH and/or FSH but do not include the GnRH receptor binding mechanisms. Our goal is to couple such a PK/PD model with the model of the female menstrual cycle.

The paper is organized as follows. In Sec. 2 we derive the model equations with special focus on the GnRH receptor binding model and the coupling of a PK model. The problem of parameter identification is addressed in Sec. 3. Sec. 4 contains the simulation results for the normal cycle as well as for the treatment with Nafarelin and Cetrorelix. The conclusion follows in Sec. 5. Details about initial values and parameter values as well as a list of abbreviations are shifted to the appendix.

2 Model Equations

The model of the female menstrual cycle includes the physiological compartments hypothalamus, pituitary gland and ovaries, connected by the bloodstream. The model delivers a qualitative description of the following regulatory circuit as illustrated in the flowchart in Fig. 1: In the hypothalamus, the hormone GnRH (gonadotropin-releasing hormone) is formed, which reaches the pituitary gland through a portal system and stimulates the release of the gonadotropins LH and FSH into the bloodstream. The gonadotropins regulate the processes in the ovaries, i.e. the multi-stage maturation process of the follicles, ovulation and the development of the corpus luteum, which control the synthesis of the steroids P4 and E2 and of the hormones IhA and IhB. Through the blood, these hormones then reach the hypothalamus and pituitary gland, where they again influence the formation of GnRH, LH and FSH.

Since exact mechanisms are often unknown or more specific than necessary, Hill functions are

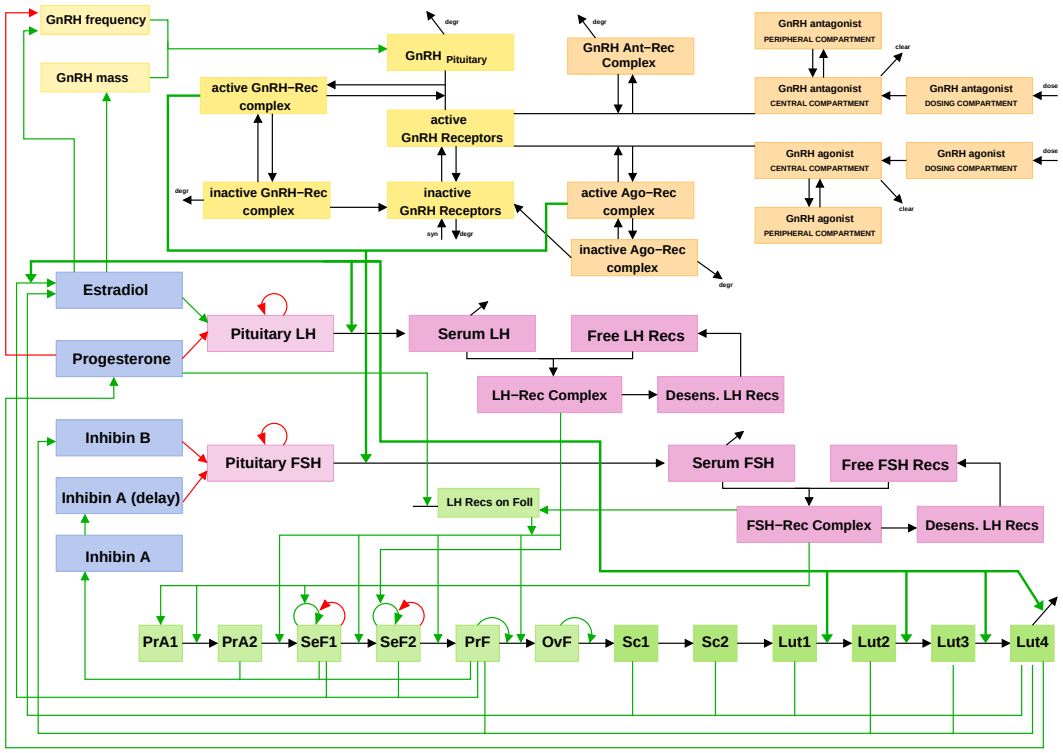

Figure 1: Flowchart of the model for the female menstrual cycle.

used to model stimulatory (H^+) or inhibitory (H^-) effects:

$$H^+(S(t),T;n) = \frac{(S(t)/T)^n}{1+(S(t)/T)^n}, \quad H^-(S(t),T;n) = \frac{1}{1+(S(t)/T)^n}.$$

Here, $S(t) \geq 0$ denotes the influencing substance, $T > 0$ the threshold, and $n \geq 1$ the Hill coefficient, which determines the rate of switching.

The following model equations partially overlap with equations used in the models of Harris [16], Pasteur [30] and Reinecke [31], but have been extended and adapted for the purpose of simulating GnRH analogue treatment. We started with the Reinecke model (named "original" model) and performed model extension and reduction. First, we reduced this model by omitting components which couple only weakly to the rest of the model. In particular, we left out the enzyme reactions in the ovaries. According to [30], the number of follicular phases was extended from 5 to 8 in order to distinguish between IhA and IhB. Moreover, we replaced the stochastic GnRH pulse generator by a deterministic counterpart, which will be explained in more detail in Sec. 2.5.

2.1 Luteinizing Hormone

The gonadotropin equations are based on synthesis-release-clearance relationships. This structure was first introduced in [33]. LH-synthesis in the pituitary is stimulated by E2 and inhibited by P4. There is a small constant release rate of LH into the blood ($b_{\mathrm{LH}_{Rel}}$) [19], but the release is mainly stimulated by the GnRH-receptor complex and additionally, if present, by the agonist-receptor complex. Parameter V_{blood} corresponds to the blood volume. From the blood, LH is cleared by

binding to free LH receptors (k_{on}^{LH}) and by other unspecified mechanisms (cl_{LH}) .

$$Syn_{\mathrm{LH}}(t) = (b_{\mathrm{LH}_{Syn}} + m_{\mathrm{E2}}^{\mathrm{LH}} \cdot H^{+}(\mathrm{E2}(t), T_{\mathrm{E2}}^{\mathrm{LH}}; n_{\mathrm{E2}}^{\mathrm{LH}})) \cdot H^{-}(\mathrm{P4}(t), T_{\mathrm{P4}}^{\mathrm{LH}}; n_{\mathrm{P4}}^{\mathrm{LH}}) \tag{1a}$$

$$Rel_{\mathrm{LH}}(t) = \left(b_{\mathrm{LH}_{Rel}} + m_{\mathrm{G\text{-}R}}^{\mathrm{LH}} \cdot H^{+}(\mathrm{G\text{-}R}(t) + \mathrm{Ago\text{-}R}(t), T_{\mathrm{G\text{-}R}}^{\mathrm{LH}}; n_{\mathrm{G\text{-}R}}^{\mathrm{LH}})\right) \cdot \mathrm{LH}_{\mathrm{pit}}(t) \tag{1b}$$

$$\frac{d}{dt}\mathrm{LH}_{\mathrm{pit}}(t) = Syn_{\mathrm{LH}}(t) - Rel_{\mathrm{LH}}(t) \tag{1}$$

$$\frac{d}{dt}\mathrm{LH}_{blood}(t) = \frac{1}{V_{blood}} \cdot Rel_{\mathrm{LH}}(t) - (k_{on}^{\mathrm{LH}} \cdot \mathrm{R}_{\mathrm{LH}}(t) + cl_{\mathrm{LH}}) \cdot \mathrm{LH}_{blood}(t) \tag{2}$$

LH receptor binding is described by chemical reaction kinetics:

$$\begin{aligned} \mathrm{LH}_{blood} + \mathrm{R}_{\mathrm{LH}} &\xrightarrow{k_{on}^{\mathrm{LH}}} \mathrm{LH\text{-}R} \\ \mathrm{LH\text{-}R} &\xrightarrow{k_{des}^{\mathrm{LH}}} \mathrm{R}_{\mathrm{LH},des} \\ \mathrm{R}_{\mathrm{LH},des} &\xrightarrow{k_{recy}^{\mathrm{LH}}} \mathrm{R}_{\mathrm{LH}} \end{aligned}$$

The corresponding differential equations read:

$$\frac{d}{dt}\mathrm{R}_{\mathrm{LH}}(t) = k_{recy}^{\mathrm{LH}} \cdot \mathrm{R}_{\mathrm{LH},des}(t) - k_{on}^{\mathrm{LH}} \cdot \mathrm{LH}_{blood}(t) \cdot \mathrm{R}_{\mathrm{LH}}(t) \tag{3}$$

$$\frac{d}{dt}\mathrm{LH\text{-}R}(t) = k_{on}^{\mathrm{LH}} \cdot \mathrm{LH}_{blood}(t) \cdot \mathrm{R}_{\mathrm{LH}}(t) - k_{des}^{\mathrm{LH}} \cdot \mathrm{LH\text{-}R}(t) \tag{4}$$

$$\frac{d}{dt}\mathrm{R}_{\mathrm{LH},des}(t) = k_{des}^{\mathrm{LH}} \cdot \mathrm{LH\text{-}R}(t) - k_{recy}^{\mathrm{LH}}(t) \cdot \mathrm{R}_{\mathrm{LH},des}(t) \tag{5}$$

2.2 Follicle Stimulating Hormone

FSH synthesis is stimulated by low GnRH frequencies to account for a suppression of FSH in case of a constant frequency [15]. Moreover, FSH synthesis is inhibited by IhA and IhB [14, 18, 24, 34]. In [30], these mechanisms were modelled by delay differential equations to account for a delayed inhibitory effect of both IhA and IhB. Since in our model the timing of FSH synthesis and release is additionally influenced by GnRH, the delayed effect of IhB could be neglected. The delayed effect of IhA, however, is still important. To avoid the use of delay differential equations we therefore introduced a "delay component" IhA_{τ}, compare Eq. (28). The equations for release and clearance of FSH are the same as for LH.

$$Syn_{\mathrm{FSH}}(t) = \frac{m_{\mathrm{Ih}}^{\mathrm{FSH}}}{1 + \left(\frac{\mathrm{IhA}_{\tau}}{T_{\mathrm{IhA}}}\right)^{n_{\mathrm{IhA}}} + \left(\frac{\mathrm{IhB}}{T_{\mathrm{IhB}}}\right)^{n_{\mathrm{IhB}}}} \cdot H^{-}(\mathrm{freq}, T_{\mathrm{freq}}^{\mathrm{FSH}}; n_{\mathrm{freq}}^{\mathrm{FSH}}) \tag{6a}$$

$$Rel_{\mathrm{FSH}}(t) = \left(b_{\mathrm{FSH}_{Rel}} + m_{\mathrm{G\text{-}R}}^{\mathrm{FSH}} \cdot H^{+}(\mathrm{G\text{-}R}(t) + \mathrm{Ago\text{-}R}(t), T_{\mathrm{G\text{-}R}}^{\mathrm{FSH}}; n_{\mathrm{G\text{-}R}}^{\mathrm{FSH}})\right) \cdot \mathrm{FSH}_{\mathrm{pit}}(t) \tag{6b}$$

$$\frac{d}{dt}\mathrm{FSH}_{\mathrm{pit}}(t) = Syn_{\mathrm{FSH}}(t) - Rel_{\mathrm{FSH}}(t) \tag{6}$$

$$\frac{d}{dt}\mathrm{FSH}_{blood}(t) = \frac{1}{V_{blood}} \cdot Rel_{\mathrm{FSH}}(t) - (k_{on}^{\mathrm{FSH}} \cdot \mathrm{R}_{\mathrm{FSH}} + cl_{\mathrm{FSH}}) \cdot \mathrm{FSH}_{blood}(t) \tag{7}$$

FSH receptor binding is described by chemical reaction kinetics:

$$\begin{aligned} \mathrm{FSH}_{blood} + \mathrm{R}_{\mathrm{FSH}} &\xrightarrow{k_{on}^{\mathrm{FSH}}} \mathrm{FSH\text{-}R}_{\mathrm{FSH}} \\ \mathrm{FSH\text{-}R}_{\mathrm{FSH}} &\xrightarrow{k_{des}^{\mathrm{FSH}}} \mathrm{R}_{\mathrm{FSH},des} \\ \mathrm{R}_{\mathrm{FSH},des} &\xrightarrow{k_{recy}^{\mathrm{FSH}}} \mathrm{R}_{\mathrm{FSH}} \end{aligned}$$

The corresponding differential equations read:

$$\frac{d}{dt}\mathrm{R_{FSH}}(t) = k_{recy}^{\mathrm{FSH}} \cdot \mathrm{R_{FSH},}_{des}(t) - k_{on}^{\mathrm{FSH}} \cdot \mathrm{FSH}_{blood}(t) \cdot \mathrm{R_{FSH}}(t) \tag{8}$$

$$\frac{d}{dt}\mathrm{FSH\text{-}R}(t) = k_{on}^{\mathrm{FSH}} \cdot \mathrm{FSH}_{blood}(t) \cdot \mathrm{R_{FSH}}(t) - k_{des}^{\mathrm{FSH}} \cdot \mathrm{FSH\text{-}R}(t) \tag{9}$$

$$\frac{d}{dt}\mathrm{R_{FSH},}_{des}(t) = k_{des}^{\mathrm{FSH}} \cdot \mathrm{FSH\text{-}R}(t) - k_{recy}^{\mathrm{FSH}} \cdot \mathrm{R_{FSH},}_{des}(t) \tag{10}$$

2.3 Development of Follicles and Corpus Luteum

The model for the development of follicles is adapted from [30]. Follicular growth is initiated by FSH. Then, transition from one follicular stage to the next is stimulated by LH and/or FSH. Moreover, the growth rate of the secondary follicles SeF1 and SeF2 increases with increasing follicle size. To account for large LH and FSH peaks resulting from GnRH agonist treatment, we added some new features to the original model.

First, the action of LH and FSH was replaced by the action of their corresponding receptor complexes. Moreover, the growth of the secondary follicles SeF1 and SeF2 is now bounded by a maximum capacity ($SeF_{\max}$). With increasing size, the follicles evolve LH-receptors ($\mathrm{R_{LH}^{foll}}$) on the granulosa cells, thus becoming more sensitive to LH, which stimulates their transition to the next stage [39]. The LH receptors disappear with the sustained development of the corpus luteum, represented by increasing amounts of P4:

$$\frac{d}{dt}\mathrm{R_{LH}^{foll}}(t) = m_{\mathrm{FSH}}^{\mathrm{R_{LH}}} \cdot H^{+}(\mathrm{FSH\text{-}R}(t), T_{\mathrm{FSH}}^{\mathrm{R_{LH}}}; n_{\mathrm{FSH}}^{\mathrm{R_{LH}}}) - m_{\mathrm{P4}}^{\mathrm{R_{LH}}} \cdot H^{+}(\mathrm{P4}(t), T_{\mathrm{P4}}^{\mathrm{R_{LH}}}; n_{\mathrm{P4}}^{\mathrm{R_{LH}}}) \cdot \mathrm{R_{LH}^{foll}}(t) \tag{11}$$

All LH dependent transition rates between different follicular stages are multiplied with the amount of $\mathrm{R_{LH}^{foll}}$. These changes became necessary to capture different effects of an LH peak (caused by GnRH agonist treatment) in the early and late follicular phase. The corpus luteum starts to develop under the condition that there is an LH peak and the follicles are ready for ovulation. Therefore an ovulatory follicle (OvF) only develops when the preovulatory follicle (PrF) is large enough. Thus, an LH peak in the early follicular phase cannot cause ovulation. To make the ovulatory scar (Sc1) independent from the size of the ovulatory follicle OvF, its growth only depends on OvF via a Hill function. Thus, a normal luteal function is maintained even if ovulation is enforced earlier, for example by GnRH agonist treatment in the late follicular phase. Furthermore, the transitions between different luteal stages are stimulated by the GnRH-receptor complex or the agonist-receptor complex, respectively. This modification became necessary to account for a truncated luteal phase after agonist administration in the late luteal phase.

$$\frac{d}{dt}\mathrm{PrA1}(t) = m_{\mathrm{FSH}}^{\mathrm{PrA1}} \cdot H^{+}(\mathrm{FSH\text{-}R}(t), T_{\mathrm{FSH}}^{\mathrm{PrA1}}; n_{\mathrm{FSH}}^{\mathrm{PrA1}}) - k_{\mathrm{PrA1}}^{\mathrm{PrA2}} \cdot \mathrm{FSH\text{-}R}(t) \cdot \mathrm{PrA1}(t) \tag{12}$$

$$\begin{aligned}\frac{d}{dt}\mathrm{PrA2}(t) = {} & k_{\mathrm{PrA1}}^{\mathrm{PrA2}} \cdot \mathrm{FSH\text{-}R}(t) \cdot \mathrm{PrA1}(t) \\ & - k_{\mathrm{PrA2}}^{\mathrm{SeF1}} \cdot (\mathrm{LH\text{-}R}(t)/SF_{\mathrm{LH\text{-}R}})^{n_{\mathrm{PrA2}}^{\mathrm{SeF1}}} \cdot \mathrm{R^{foll}}(t)_{\mathrm{LH}} \cdot \mathrm{PrA2}(t)\end{aligned} \tag{13}$$

$$\begin{aligned}\frac{d}{dt}\mathrm{SeF1}(t) = {} & k_{\mathrm{PrA2}}^{\mathrm{SeF1}} \cdot (\mathrm{LH\text{-}R}(t)/SF_{\mathrm{LH\text{-}R}})^{n_{\mathrm{PrA2}}^{\mathrm{SeF1}}} \cdot \mathrm{R_{LH}^{foll}}(t) \cdot \mathrm{PrA2}(t) \\ & + k_{\mathrm{SeF1}}^{\mathrm{SeF1}} \cdot \mathrm{FSH\text{-}R}(t) \cdot \mathrm{SeF1}(t) \cdot (1 - \mathrm{SeF1}(t)/SeF_{\max}) \\ & - k_{\mathrm{SeF1}}^{\mathrm{SeF2}} \cdot (\mathrm{LH\text{-}R}(t)/SF_{\mathrm{LH\text{-}R}})^{n_{\mathrm{SeF1}}^{\mathrm{SeF2}}} \cdot \mathrm{R_{LH}^{foll}}(t) \cdot \mathrm{SeF1}(t)\end{aligned} \tag{14}$$

$$\begin{aligned}\frac{d}{dt}\mathrm{SeF2}(t) = {} & k_{\mathrm{SeF1}}^{\mathrm{SeF2}} \cdot (\mathrm{LH\text{-}R}(t)/SF_{\mathrm{LH\text{-}R}})^{n_{\mathrm{SeF1}}^{\mathrm{SeF2}}} \cdot \mathrm{R_{LH}^{foll}}(t) \cdot \mathrm{SeF1}(t) \\ & + k_{\mathrm{SeF2}}^{\mathrm{SeF2}} \cdot (\mathrm{LH\text{-}R}(t)/SF_{\mathrm{LH\text{-}R}})^{n_{\mathrm{SeF2}}} \cdot \mathrm{SeF2}(t) \cdot (1 - \mathrm{SeF2}(t)/SeF_{\max}) \\ & - k_{\mathrm{SeF2}}^{\mathrm{PrF}} \cdot (\mathrm{LH\text{-}R}(t)/SF_{\mathrm{LH\text{-}R}}) \cdot \mathrm{R_{LH}^{foll}}(t) \cdot \mathrm{SeF2}(t)\end{aligned} \tag{15}$$

$$\frac{d}{dt}\mathrm{PrF}(t) = k^{\mathrm{PrF}}_{\mathrm{SeF2}} \cdot (\text{LH-R}(t)/SF_{\text{LH-R}}) \cdot \mathrm{R}^{\mathrm{foll}}_{\mathrm{LH}}(t) \cdot \mathrm{SeF2}(t) - cl_{\mathrm{PrF}} \cdot (\text{LH-R}(t)/SF_{\text{LH-R}})^{n^{\mathrm{OvF}}_{\mathrm{PrF}}} \cdot \mathrm{R}^{\mathrm{foll}}_{\mathrm{LH}}(t) \cdot \mathrm{PrF}(t) \tag{16}$$

$$\frac{d}{dt}\mathrm{OvF}(t) = m^{\mathrm{OvF}}_{\mathrm{PrF}} \cdot (\text{LH-R}(t)/SF_{\text{LH-R}})^{n^{\mathrm{OvF}}_{\mathrm{PrF}}} \cdot \mathrm{R}^{\mathrm{foll}}_{\mathrm{LH}}(t) \cdot H^+(\mathrm{PrF}(t), T^{\mathrm{OvF}}_{\mathrm{PrF}}; n^{\mathrm{OvF}}_{\mathrm{PrF}}) - cl_{\mathrm{OvF}} \cdot \mathrm{OvF}(t) \tag{17}$$

$$\frac{d}{dt}\mathrm{Sc1}(t) = m^{\mathrm{Sc1}}_{\mathrm{OvF}} \cdot H^+(\mathrm{OvF}(t), T^{\mathrm{Sc1}}_{\mathrm{OvF}}, n^{\mathrm{Sc1}}_{\mathrm{OvF}}) - k^{\mathrm{Sc2}}_{\mathrm{Sc1}} \cdot \mathrm{Sc1}(t) \tag{18}$$

$$\frac{d}{dt}\mathrm{Sc2}(t) = k^{\mathrm{Sc2}}_{\mathrm{Sc1}} \cdot \mathrm{Sc1}(t) - k^{\mathrm{Lut1}}_{\mathrm{Sc2}} \cdot \mathrm{Sc2}(t) \tag{19}$$

$$\frac{d}{dt}\mathrm{Lut1}(t) = k^{\mathrm{Lut1}}_{\mathrm{Sc2}} \cdot \mathrm{Sc2}(t) - k^{\mathrm{Lut2}}_{\mathrm{Lut1}} \cdot (1 + m^{\mathrm{Lut}}_{\text{G-R}} \cdot H^+(\text{G-R}(t) + \text{Ago-R}(t), T^{\mathrm{Lut}}_{\text{G-R}}; n^{\mathrm{Lut}}_{\text{G-R}})) \cdot \mathrm{Lut1}(t) \tag{20}$$

$$\frac{d}{dt}\mathrm{Lut2}(t) = k^{\mathrm{Lut2}}_{\mathrm{Lut1}} \cdot (1 + m^{\mathrm{Lut}}_{\text{G-R}} \cdot H^+(\text{G-R}(t) + \text{Ago-R}(t), T^{\mathrm{Lut}}_{\text{G-R}}; n^{\mathrm{Lut}}_{\text{G-R}})) \cdot \mathrm{Lut1}(t) - k^{\mathrm{Lut3}}_{\mathrm{Lut2}} \cdot (1 + m^{\mathrm{Lut}}_{\text{G-R}} \cdot H^+(\text{G-R}(t) + \text{Ago-R}(t), T^{\mathrm{Lut}}_{\text{G-R}}; n^{\mathrm{Lut}}_{\text{G-R}})) \cdot \mathrm{Lut2}(t) \tag{21}$$

$$\frac{d}{dt}\mathrm{Lut3}(t) = k^{\mathrm{Lut3}}_{\mathrm{Lut2}}(1 + m^{\mathrm{Lut}}_{\text{G-R}} \cdot H^+(\text{G-R}(t) + \text{Ago-R}(t), T^{\mathrm{Lut}}_{\text{G-R}}; n^{\mathrm{Lut}}_{\text{G-R}})) \cdot \mathrm{Lut2}(t) - k^{\mathrm{Lut4}}_{\mathrm{Lut3}} \cdot (1 + m^{\mathrm{Lut}}_{\text{G-R}} \cdot H^+(\text{G-R}(t) + \text{Ago-R}(t), T^{\mathrm{Lut}}_{\text{G-R}}; n^{\mathrm{Lut}}_{\text{G-R}})) \cdot \mathrm{Lut3}(t) \tag{22}$$

$$\frac{d}{dt}\mathrm{Lut4}(t) = k^{\mathrm{Lut4}}_{\mathrm{Lut3}}(1 + m^{\mathrm{Lut}}_{\text{G-R}} \cdot H^+(\text{G-R}(t) + \text{Ago-R}(t), T^{\mathrm{Lut}}_{\text{G-R}}; n^{\mathrm{Lut}}_{\text{G-R}})) \cdot \mathrm{Lut3}(t) - cl_{\mathrm{Lut4}} \cdot (1 + m^{\mathrm{Lut}}_{\text{G-R}} \cdot H^+(\text{G-R}(t) + \text{Ago-R}(t), T^{\mathrm{Lut}}_{\text{G-R}}; n^{\mathrm{Lut}}_{\text{G-R}})) \cdot \mathrm{Lut4}(t) \tag{23}$$

2.4 Estradiol, Progesterone and Inhibins

E2, P4, IhA and IhB are produced by the follicles and/or the corpus luteum. The ability of the follicles to produce E2 is stimulated by the GnRH-receptor complex and additionally, if present, by the agonist-receptor complex. This feature was introduced in the model to capture the increase in E2 at agonist administration.

$$\frac{d}{dt}\mathrm{E2}(t) = b_{\mathrm{E2}} + k^{\mathrm{E2}}_{\mathrm{SeF1}} \cdot (\text{G-R}(t) + \text{Ago-R}(t)) \cdot \mathrm{SeF1}(t) + k^{\mathrm{E2}}_{\mathrm{SeF2}} \cdot \mathrm{SeF2}(t) + k^{\mathrm{E2}}_{\mathrm{PrF}} \cdot (\text{G-R}(t) + \text{Ago-R}(t)) \cdot \mathrm{PrF} + k^{\mathrm{E2}}_{\mathrm{Lut1}} \cdot \mathrm{Lut1}(t) + k^{\mathrm{E2}}_{\mathrm{Lut4}} \cdot \mathrm{Lut4}(t) - cl_{\mathrm{E2}} \cdot \mathrm{E2}(t) \tag{24}$$

$$\frac{d}{dt}\mathrm{P4}(t) = b_{\mathrm{P4}} + k^{\mathrm{P4}}_{\mathrm{Lut4}} \cdot \mathrm{Lut4}(t) - cl_{\mathrm{P4}} \cdot \mathrm{P4}(t) \tag{25}$$

$$\frac{d}{dt}\mathrm{IhA}(t) = b_{\mathrm{IhA}} + k^{\mathrm{IhA}}_{\mathrm{PrF}} \cdot \mathrm{PrF}(t) + k^{\mathrm{IhA}}_{\mathrm{Lut2}} \cdot \mathrm{Lut2}(t) + k^{\mathrm{IhA}}_{\mathrm{Lut3}} \cdot \mathrm{Lut3}(t) + k^{\mathrm{IhA}}_{\mathrm{Lut4}} \cdot \mathrm{Lut4}(t) - cl_{\mathrm{IhA}} \cdot \mathrm{IhA}(t) \tag{26}$$

$$\frac{d}{dt}\mathrm{IhB}(t) = b_{\mathrm{IhB}}(t) + k^{\mathrm{IhB}}_{\mathrm{PrA2}} \cdot \mathrm{PrA2}(t) + k^{\mathrm{IhB}}_{\mathrm{Sc2}} \cdot \mathrm{Sc2}(t) - cl_{\mathrm{IhB}} \cdot \mathrm{IhB}(t) \tag{27}$$

To account for a delayed effect of IhA on FSH synthesis and to avoid the use of delay differential equations, we additionally introduce a "delay component":

$$\frac{d}{dt}\mathrm{IhA}_\tau(t) = cl_{\mathrm{IhA}} \cdot \mathrm{IhA}(t) - cl_{\mathrm{IhA}_\tau}\mathrm{IhA}_\tau \tag{28}$$

2.5 Gonadotropin Releasing Hormone

The level of GnRH (G) is dependent on the amount (mass) produced in the hypothalamus and the frequency of pulsatile release into the pituitary. The frequency is inhibited by P4 and stimulated

by E2 [13, 21, 15]. Moreover, we assume that E2 is inhibitory on the released amount of GnRH at low concentrations and stimulatory at high concentrations [4, 37, 15].

$$\text{freq}(t) = k^{freq} H^{-}(\text{P4}(t), T_{\text{P4}}^{\text{freq}}; n_{\text{P4}}^{\text{freq}}) \cdot (1 + m_{\text{E2}}^{\text{freq}} \cdot H^{+}(\text{E2}(t), T_{\text{E2}}^{\text{freq}}; n_{\text{E2}}^{\text{freq}})) \tag{29a}$$

$$\text{mass}(t) = k^{mass} \left(H^{+}(\text{E2}(t), T_{\text{E2}}^{\text{mass},1}; n_{\text{E2}}^{\text{mass},1}) + H^{-}(\text{E2}(t), T_{\text{E2}}^{\text{mass},2}; n_{\text{E2}}^{\text{mass},2}) \right) \tag{29b}$$

$$\frac{d}{dt}\text{G}(t) = \text{mass}(t) \cdot \text{freq}(t) - k_{on}^{G} \cdot \text{G}(t) \cdot \text{R}_{\text{G,a}}(t) + k_{off}^{G} \cdot \text{G-R}_a(t) - k_{degr}^{G} \cdot \text{G}(t) \tag{29}$$

This modelling is purely deterministic, in contrast to the stochastic GnRH pulse generator that was used by Reinecke [32]. That stochastic modelling, when correctly implemented, had required extremely small time steps which are impractical for the simulation of several cycles including parameter identification. Moreover, in that model a constant GnRH pulse frequency had had no effect on the course of the menstrual cycle, which contradicts scientific findings. Since we are not interested in the stochastic pulse pattern but in the mean frequency and the amount of GnRH in the pituitary, the deterministic modelling is fully sufficient. If wanted, the pulse pattern of GnRH could be computed from the frequency but this is not in the scope of our present model.

The model for the GnRH receptor binding is similar to the model of the epidermal growth factor receptor presented in [22] and is described via the following scheme:

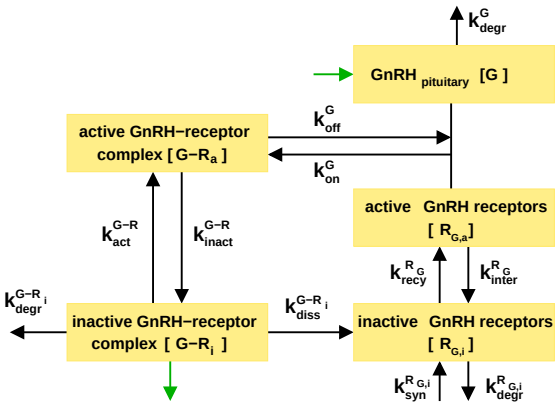

Figure 2: GnRH receptor binding model as it is integrated into the large model, see upper left part of Fig. 1.

In the pituitary, the GnRH receptors available for binding ($\text{R}_{\text{G,a}}$) are assumed to be on the cell surface. We also assume a pool of inactive GnRH receptors ($\text{R}_{\text{G,i}}$) inside the cell, not available for binding. The GnRH that is released from the hypothalamus binds via a reversible reaction to its free receptors on the cell surface, forming an active GnRH-receptor complex (G-R_a), that is also located on the cell surface. This complex gets internalized (or inactivated) and recycled to the membrane (re-activated) in a reversible way. The inactive complex (G-R_i) is degraded and, at the same time, it dissociates inside the cell, forming new inactive GnRH receptors in the pool. From the pool, a certain amount of receptors are permanently recycled and becoming active with rate constant $k_{recy}^{\text{R}_\text{G}}$. At the same time active receptors on the cell surface are internalised and become inactive with rate constant $k_{inter}^{\text{R}_\text{G}}$. We assume that there is a permanent synthesis and degradation of free inactive receptors inside the cell. The differential equations corresponding to

the above described reaction scheme are described below:

$$\frac{d}{dt}\mathrm{R_{G,a}}(t) = k_{off}^{G} \cdot \text{G-R}_a(t) - k_{on}^{G} \cdot \mathrm{G}(t) \cdot \mathrm{R_{G,a}}(t) - k_{inter}^{\mathrm{R_G}} \cdot \mathrm{R_{G,a}}(t) + k_{recy}^{\mathrm{R_G}} \mathrm{R_{G,i}} \tag{30*}$$

$$\frac{d}{dt}\mathrm{R_{G,i}}(t) = k_{diss}^{\text{G-R}_i} \cdot \text{G-R}_i(t) + k_{inter}^{\mathrm{R_G}} \cdot \mathrm{R_{G,a}}(t) - k_{recy}^{\mathrm{R_G}} \mathrm{R_{G,i}}(t) + k_{syn}^{\mathrm{R_{G,i}}} - k_{degr}^{\mathrm{R_{G,i}}} \cdot \mathrm{R_{G,i}}(t) \tag{31*}$$

$$\frac{d}{dt}\text{G-R}_a(t) = k_{on}^{G} \cdot \mathrm{G}(t) \cdot \mathrm{R_{G,a}}(t) - k_{off}^{G} \cdot \text{G-R}_a(t) - k_{inact}^{\text{G-R}} \cdot \text{G-R}_a(t) + k_{act}^{\text{G-R}} \text{G-R}_i(t) \tag{32}$$

$$\frac{d}{dt}\text{G-R}_i(t) = k_{inact}^{\text{G-R}} \cdot \text{G-R}_a(t) - k_{act}^{\text{G-R}} \text{G-R}_i(t) - k_{degr}^{\text{G-R}_i} \cdot \text{G-R}_i(t) - k_{diss}^{\text{G-R}_i} \cdot \text{G-R}_i(t) \tag{33}$$

The star in the equation number labels preliminary equations which are changed when GnRH analogues are included into the model system.

2.6 Administration of GnRH Analogues

2.6.1 The pharmacokinetic model

Administration of GnRH agonists and antagonists is modelled via a classical two-compartment-PK model [3]. The drug is administered directly into the dosing compartment, from where it is transported into the central compartment. A certain amount of drug reaches the peripheral compartment, from where it is transported back into the central compartment. We chose this approach to account for a two-phase decrease in the drug data (Cetrorelix). Regarding the data of Nafarelin, the agonist model could as well be modelled with a one-compartment-PK model, but the current approach is more general and only insignificantly more costly. In the following, we use the agonist as example to describe the reaction scheme between the compartments:

$$\mathrm{Ago_d} \xrightarrow{k_A^{Ago}} \mathrm{Ago_c} \underset{k_{pc}^{Ago}}{\overset{k_{cp}^{Ago}}{\rightleftharpoons}} \mathrm{Ago_p} \quad , \qquad \mathrm{Ago_c} \xrightarrow{cl_{\mathrm{Ago_c}}} *$$

$\mathrm{Ago_d}$ is the amount of agonist in the dosing compartment, $\mathrm{Ago_c}$ the amount in the central, and $\mathrm{Ago_p}$ the amount in the peripheral compartment. Here and in the following, the $*$ represents a component without feedback to the rest of the system, which is therefore neglected during the simulation.

The agonist concentration in the dosing compartment is determined by first order absorption:

$$\frac{d}{dt}\mathrm{Ago_d}(t) = -k_A^{Ago} \cdot \mathrm{Ago_d}(t) \tag{34}$$

At the time points of dosing, $\{t_{D,i}\}_{i=1}^{n}$, the dose D_{Ago} is added to $\mathrm{Ago_d}(t)$.

Since only the free drug in the central compartment is available for binding to the GnRH receptor, we multiply the amount of agonist that reaches the central compartment from the dosing compartment with the fraction unbound in plasma, f_u^{Ago}. This value was obtained from the literature [25, 28]. Moreover, the agonist concentration is diluted with respect to the volume of the central compartment (V_c).

The differential equations for the components of the PK model are:

$$\begin{aligned}\frac{d}{dt}\mathrm{Ago_c}(t) = {} & k_A^{Ago} \cdot \mathrm{Ago_d}(t) \cdot f_u^{Ago}/V_c - cl_{Ago_c} \cdot \mathrm{Ago_c}(t) \\ & - k_{cp}^{Ago} \cdot \mathrm{Ago_c}(t) + k_{pc}^{Ago} \cdot \mathrm{Ago_p}(t)\end{aligned} \tag{35*}$$

$$\frac{d}{dt}\mathrm{Ago_p}(t) = k_{cp}^{Ago} \cdot \mathrm{Ago_c}(t) - k_{pc}^{Ago} \cdot \mathrm{Ago_p}(t) \tag{36}$$

The equations for the antagonist PK model look exactly the same, except that in the parameter and component names “Ago” is replaced by “Ant”.

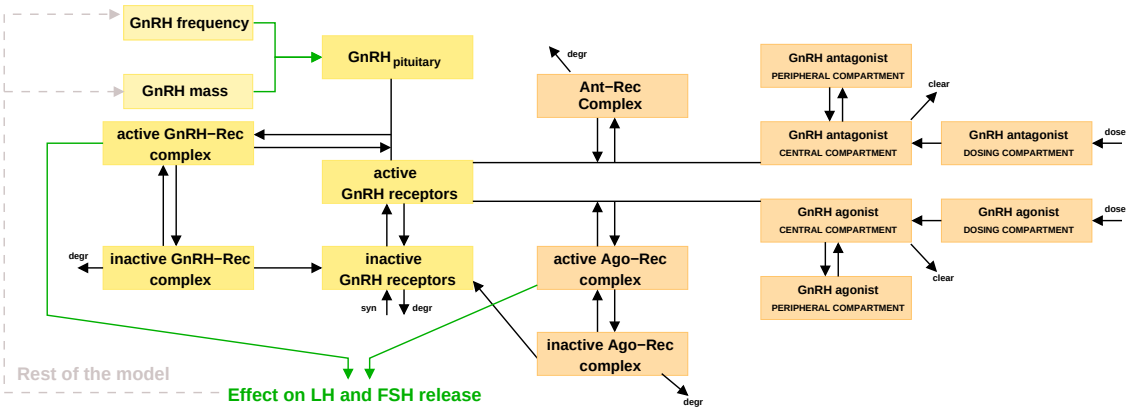

Figure 3: Coupling of the 2-compartment PK model to the GnRH receptor binding model, see also upper part of Fig. 1.

2.6.2 Agonist receptor binding

The coupling of the PK equations to the rest of the model occurs via reaction-rate equations (Fig. 3). The agonist binds via a reversible reaction to free GnRH receptors on the cell surface ($\mathrm{R_{G,a}}$) and forms an active complex (Ago-R_a), which is acting in the same way as the GnRH-receptor complex. That means, the complex gets internalized and recycled in a reversible way. The inactive complex is degraded or dissociated into a pool of inactive receptors inside the cell. The reaction scheme is:

$$SF_{\mathrm{Ago}} \cdot \mathrm{Ago_c} + \mathrm{R_{G,a}} \underset{k_{off}^{Ago}}{\overset{k_{on}^{Ago}}{\rightleftharpoons}} \text{Ago-R}_a \qquad \text{Ago-R}_a \underset{k_{inact}^{\text{Ago-R}}}{\overset{k_{act}^{\text{Ago-R}}}{\rightleftharpoons}} \text{Ago-R}_i$$

$$\text{Ago-R}_i \xrightarrow{k_{degr}^{\text{Ago-R}}} * \qquad \text{Ago-R}_i \xrightarrow{k_{diss}^{\text{Ago-R}}} \mathrm{R_{G,i}}$$

The scaling factor SF_{Ago} accounts for the conversion of units from the agonist in the central compartment (usually ng/mL) to the amount of agonist-receptor complex (nmol/mL). The amount of active and inactive agonist-receptor complex is calculated as:

$$\begin{aligned}\frac{d}{dt}\text{Ago-R}_a(t) &= k_{on}^{Ago} \cdot SF_{\mathrm{Ago}} \cdot \mathrm{R_{G,a}}(t) \cdot \mathrm{Ago_c}(t) - k_{off}^{Ago} \cdot \text{Ago-R}_a(t) \\ &\quad + k_{act}^{\text{Ago-R}} \cdot \text{Ago-R}_i(t) - k_{inact}^{\text{Ago-R}} \cdot \mathrm{R_{G,a}}(t) \cdot \text{Ago-R}_a(t) \qquad (37)\\ \frac{d}{dt}\text{Ago-R}_i(t) &= k_{inact}^{\text{Ago-R}} \cdot \mathrm{R_{G,a}}(t) \cdot \text{Ago-R}_a(t) - k_{act}^{\text{Ago-R}} \cdot \text{Ago-R}_i(t) \\ &\quad - k_{diss}^{\text{Ago-R}} \cdot \text{Ago-R}_i(t) - k_{degr}^{\text{Ago-R}} \cdot \text{Ago-R}_i(t) \qquad (38)\end{aligned}$$

The effect of the agonist-receptor-complex is added to the effect of the GnRH-receptor complex wherever it appears (cf. Rel_{LH}, Rel_{FSH}, CL development, E2).

Since the binding is reversible, it also effects the equation for the agonist in the central compartment:

$$\begin{aligned}\frac{d}{dt}\mathrm{Ago_c}(t) &= k_A^{Ago} \cdot \mathrm{Ago_d}(t) \cdot f_u^{Ago}/V_c - cl_{Ago_c} \cdot \mathrm{Ago_c}(t) \\ &\quad - k_{cp}^{Ago} \cdot \mathrm{Ago_c}(t) + k_{pc}^{Ago} \cdot \mathrm{Ago_p}(t) \\ &\quad - k_{on}^{Ago} \cdot \mathrm{R_{G,a}}(t) \cdot \mathrm{Ago_c}(t) + k_{off}^{Ago}/SF_{\mathrm{Ago}} \cdot \text{Ago-R}_a(t) \qquad (35)\end{aligned}$$

2.6.3 Antagonist receptor binding

There are differences in the impact of the agonist and antagonist, which are due to a different behavior of the agonist and antagonist receptor complexes. In contrast to the agonist, the GnRH receptor is not activated by binding to the antagonist. Therefore, we consider only the following reactions:

$$SF_{\mathrm{Ant}} \cdot \mathrm{Ant_c} + \mathrm{R_{G,a}} \underset{k_{off}^{Ant}}{\overset{k_{on}^{Ant}}{\rightleftharpoons}} \text{Ant-R} \qquad\qquad \text{Ant-R} \xrightarrow{k_{degr}^{Ant}} *$$

The equation for the antagonist-receptor complex is

$$\begin{aligned}\frac{d}{dt}\text{Ant-R}(t) = {} & k_{on}^{Ant} \cdot SF_{\mathrm{Ant}} \cdot \mathrm{R_{G,a}}(t) \cdot \mathrm{Ant_c}(t) \\ & - k_{off}^{Ant} \cdot \text{Ant-R}(t) - k_{degr}^{\text{Ant-R}} \cdot \text{Ant-R}(t). \end{aligned} \tag{39}$$

The modified equation for the central compartment becomes

$$\begin{aligned}\frac{d}{dt}\mathrm{Ant_c}(t) = {} & k_A^{Ant} \cdot \mathrm{Ant_d}(t) \cdot f_u^{Ant}/V_c - cl_{Ant_c} \cdot \mathrm{Ant_c}(t) \\ & - k_{cp}^{Ant} \cdot \mathrm{Ant_c}(t) + k_{pc}^{Ant} \cdot \mathrm{Ant_p}(t) \\ & - k_{on}^{Ant} \cdot \mathrm{R_{G,a}}(t) \cdot \mathrm{Ant_c}(t) + k_{off}^{Ant}/SF_{\mathrm{Ant}} \cdot \text{Ant-R}(t). \end{aligned} \tag{40}$$

Finally, the equations for both the active and the inactive GnRH receptors have to be modified:

$$\begin{aligned}\frac{d}{dt}\mathrm{R_{G,a}}(t) = {} & k_{off}^{G} \cdot \text{G-R}(t) - k_{on}^{G} \cdot \mathrm{G}(t) \cdot \mathrm{R_{G,a}}(t) \\ & - k_{inter}^{\mathrm{R_G}} \cdot \mathrm{R_{G,a}}(t) + k_{recy}^{\mathrm{R_G}} \mathrm{R_{G,i}} \\ & - k_{on}^{Ago} \cdot SF_{\mathrm{Ago}} \cdot \mathrm{Ago_c}(t) \cdot \mathrm{R_{G,a}}(t) + k_{off}^{Ago} \cdot \text{Ago-R}(t) \\ & - k_{on}^{\mathrm{Ant}} \cdot SF_{\mathrm{Ant}} \cdot \mathrm{Ant_c}(t) \cdot \mathrm{R_{G,a}}(t) + k_{off}^{Ant} \cdot \text{Ant-R}(t), \end{aligned} \tag{30}$$

$$\begin{aligned}\frac{d}{dt}\mathrm{R_{G,i}}(t) = {} & k_{diss}^{\text{G-R}_i} \cdot \text{G-R}_i(t) + k_{inter}^{\mathrm{R_G}} \cdot \mathrm{R_{G,a}}(t) - k_{recy}^{\mathrm{R_G}} \mathrm{R_{G,i}}(t) \\ & + k_{syn}^{\mathrm{R_G}} - k_{degr}^{\mathrm{R_G}} \cdot \mathrm{R_{G,i}}(t) + k_{diss}^{Ago} \cdot \text{Ago-R}_a(t) \end{aligned} \tag{31}$$

3 Applied numerical algorithms

The main difficulty is not to simulate the system, i.e. to solve the differential equations, but to identify the unknown parameters. We will briefly describe the mathematical techniques that we use for parameter identification.

Formally, the system of differential equations can be written as

$$\mathbf{y}'(t, \mathbf{p}) = f(\mathbf{y}(t, \mathbf{p}), \mathbf{p}),$$

where $\mathbf{y}(t, \mathbf{p}) = (y_1(t, \mathbf{p}), \ldots, y_n(t, \mathbf{p}))$ denotes the solution vector for a given parameter vector $\mathbf{p} = (p_1, \ldots, p_q)$. Assume there are m experimental data points varying in the selected component at different time points,

$$z_k = \hat{y}_{j_k}(t_k), \qquad k = 1, \ldots, m, \quad j_k \in \{1, \ldots, n\},$$

associated with corresponding measurement tolerances δz_k. Here $\hat{y}_{j_k}(t_k)$ denotes the measurement of component y_{j_k} at time t_k. The m to n mapping j_k assigns to every measurement time point t_k one of the n components of $\mathbf{y}$.

Parameter identification is equivalent to solving the least squares minimization problem

$$I(\mathbf{p}) = \mathbf{F}(\mathbf{p})^T \mathbf{F}(\mathbf{p}) \to \min_p,$$

where $\mathbf{F}(\mathbf{p}) = (F_1(\mathbf{p}), \ldots, F_m(\mathbf{p}))$ is a vector of length m with entries

$$F_k(\mathbf{p}) = \frac{y_{j_k}(t_k, \mathbf{p}) - z_k}{\delta z_k}.$$

That means we want to minimize the relative deviation of model and data at the measurement time points t_k. The above problem, which is highly nonlinear in $\mathbf{p}$, can be solved by affine covariant Gauss-Newton iteration, see [5], where each iteration step i requires the solution of a linear least squares problem,

$$J(\mathbf{p}^i)\Delta\mathbf{p}^i = \mathbf{F}(\mathbf{p}^i).$$

The kth row of the Jacobian $(m \times q)$-matrix $J(\mathbf{p})$ has the form

$$J(\mathbf{p})(k,:) = \nabla_{\mathbf{p}} y_{j_k}(t_k, \mathbf{p}),$$

thus representing the sensitivity of the solution $\mathbf{y}$ with respect to the parameters $\mathbf{p}$ at the time points of measurements. An analysis of the matrix $J(\mathbf{p})$ gives some hints whether the current combination of model and data will permit an actual identification of the parameters. Parameters with very small sensitivity have nearly no influence on the solution and can therefore not be estimated. In this case the entries of the corresponding column in $J(\mathbf{p})$ (and thus the weighted l_2 column norm) are almost zero. Furthermore, some of the parameters might be linearly dependent, which leads to nearly identical columns in $J(\mathbf{p})$. In both cases the matrix $J(\mathbf{p})$ will be singular or, from a numerical point of view, nearly singular.

Linearly independent parameters can be identified by analyzing their subcondition. Let us consider the QR-decomposition of $J(\mathbf{p})$. By a suitable permutation of the matrix columns of $J(\mathbf{p})$, the diagonal elements of the upper triangular matrix R can be ordered in the form $r_{11} \geq r_{22} \geq \ldots \geq r_{qq}$. The *subcondition* of parameter p_j is given by

$$\mathrm{sc}_j = r_{11}/r_{jj}.$$

Thus, the permutation of matrix columns corresponds to a new ordering of parameters according to increasing subcondition. The subcondition indicates whether a parameter can be estimated from the given data or not. Only those parameters can be estimated for which

$$\mathrm{sc}_j < 1/\epsilon,$$

where ϵ is the relative precision of the Jacobian $J(\mathbf{p})$ [6]. The above described techniques for solving a nonlinear least squares problem were first implemented in the software packages PARKIN [29, 7] and NLSCON [1, 5]. A renewed version of this software, named BioPARKIN [8], which is especially adapted to parameter identification in ordinary differential equation models, has been used throughout the study.

4 Simulation Results

4.1 Normal Cycles

The simulation results in Fig. 4 show that the current set of model parameters generates curves consistent with the data for 12 healthy women with a normal menstrual cycle. The women were synchronized at the beginning of the study. Parameters have been estimated such that the cycle length in the simulation is about 28 days throughout. Initial values have been chosen in such a way that the simulation starts on a limit cycle.

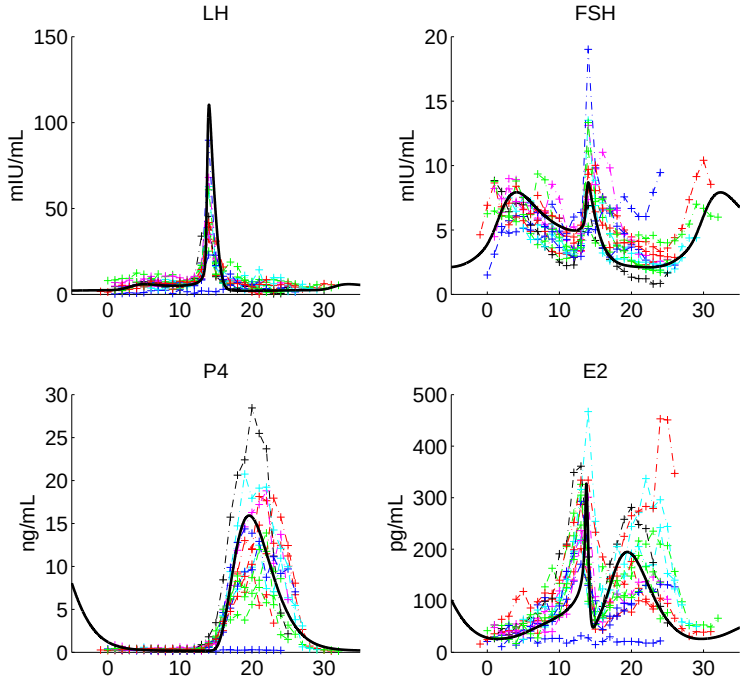

Figure 4: Simulation results (solid lines) with parameters fitted to the data from 12 healthy women (LH, FSH, E2, P4). Individual patient level hormonal data were pulled from Pfizer database. The time units are days.

4.2 GnRH Agonist Nafarelin

The parameters for the PK model of single dose Nafarelin administration were obtained as population estimates from NONMEM analysis of a 2-compartment model with 1st order absorption (Tab. 1). The values $k_{on} = 2.5\text{nM}^{-1} \cdot \text{min}^{-1}$ and $k_{off} = 5\text{min}^{-1}$ are reported in [2]. To obtain a reasonable dynamic behavior, however, we had to use values that are ten times smaller ($k_{on} = 0.25\text{nM}^{-1} \cdot \text{min}^{-1}$, $k_{off} = 0.5\text{min}^{-1}$), but the ratio $k_{on}/k_{off} = 0.5\text{nM}^{-1}$ has been kept. The remaining parameters are listed in Tab. 2. These values were used as starting values for parameter identification with single and multiple dose Nafarelin data. However, the parameters $k_{degr}^{\text{Ago-R}}$, $k_{diss}^{\text{Ago-R}}$, k_{inact}^{Ago} and k_{act}^{Ago} are difficult to estimate, see for example Fig. 5. Moreover, the values for k_{on}^{Ago} and k_{off}^{Ago} changed only slightly during optimization with data from different women. Therefore, we kept the initial parameter values because they give reasonable results. A similar argument applies to k_{on}^{Ant}, k_{off}^{Ant} and $k_{degr}^{\text{Ant-R}}$ during parameter identification with data for Cetrorelix administration. On the other hand, $cl_{\text{Ago,Ant}_c}$ is the most sensitive and best identifiable parameter. Its value for different data sets is listed in Tab. 3.

The simulation results for *single* administration of 100μg Nafarelin are illustrated in Tab. 5. Administration of Nafarelin in the early follicular phase postpones ovulation, whereas ovulation is triggered when Nafarelin is administered in the late follicular phase. The luteal phase is truncated by Nafarelin administration. Tab. 4 contains a comparison between experimental observations reported in the literature [27] and our simulation results, which are in good agreement. Similar results were obtained in a simulation with a lower dose of 5μg (figures not shown).

parameter	f_u^{A}/V_c	k_A^{A}	cl_{A_c}	k_{cp}^{A}	k_{pc}^{A}
unit	1/L	1/d	1/d	1/d	1/d
Nafarelin (sd)	0.0562	108	5.976	68.88	157.68
Cetrorelix (sd)	0.03	65.2	–	3.216	4.76
Cetrorelix (md)	0.023	73.84	–	2.704	0.936

Table 1: Pharmacokinetic parameters for single dose Nafarelin administration (NONMEM population estimates) and for the administration of single and multiple dose Cetrorelix (reported in [28]). The parameters occur in Eq. (35) and Eq. (40). The superscript letter "A" in the parameter names stands for Ant or Ago, respectively.

parameter	k_{on}^{A}	k_{off}^{A}	$k_{degr}^{\text{A-R}}$	$k_{diss}^{\text{A-R}}$	k_{inact}^{A}	k_{act}^{A}
unit	L/(d·nmol)	1/d	1/d	1/d	1/d	1/d
Nafarelin	360	720	0.1	360	0.36	3.6
Cetrorelix	360	720	0.01	–	–	–

Table 2: Receptor binding parameters for Nafarelin and Cetrorelix. The parameters occur in Eq. (37), Eq. (38), and Eq. (39). The superscript letter "A" in the parameter names stands for Ant or Ago, respectively.

The simulation results for *multiple* administration of 250μg Nafarelin are presented in Fig. 6. After the initial stimulatory phase, LH and FSH levels are suppressed but acute responses to Nafarelin are maintained. In all cases, ovulation is inhibited (absence of luteal phase). The acute E2 response is still evident, but the higher the dose, the more profound the suppression of E2 (figures not shown). This agrees very well with the observation in [26].

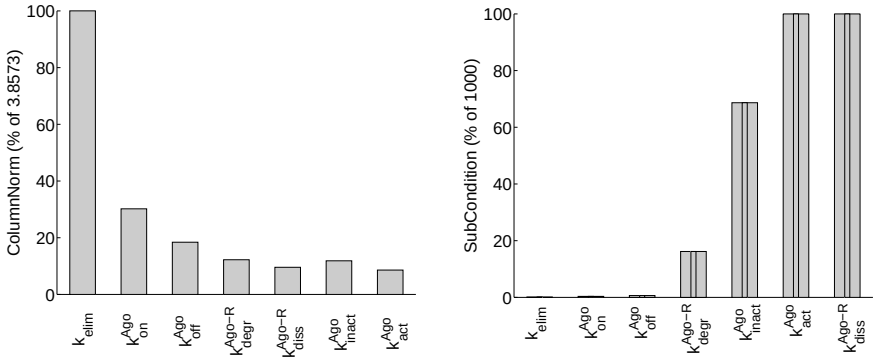

Figure 5: Information from parameter identification for selected parameters with the data for single dose Nafarelin administration (ID208). *Left:* The column norms of the sensitivity matrix show that all selected parameters are sensitive, with cl_{Ago_c} being most sensitive. *Right:* Parameters with large subcondition, however, are difficult to estimate ($k_{degr}^{\text{Ago-R}}$, k_{inact}^{Ago}) or cannot be estimated at all ($k_{diss}^{\text{Ago-R}}$, k_{act}^{Ago}) from the given data.

4.3 GnRH Antagonist Cetrorelix

The parameters for the PK model of single and multiple dose Cetrorelix administration were reported in [28], see Tab. 1. Furthermore, the data for single as well as multiple dosing can be captured equally well by the same receptor binding parameter values, see Tab. 2.

The simulations for single dose administration of Cetrorelix were performed by varying the time of dosing, the dose (D_{Ant}), and the clearance rate constant (cl_{Ant_c}), see Tab. 3. All other parameter values were kept fixed. The simulation results are illustrated in Tab. 6 and Tab. 7. High doses ($\geq 3\,\mathrm{mg}$) postpone ovulation, whereas lower doses ($\leq 1\,\mathrm{mg}$) do not result in a delay. This agrees with published data [23, 9]. In our model, the length of the suppressive effect depends on the individual clearance rate of Cetrorelix from the central compartment.

The simulation results for multiple dose administration are presented in Tab. 8. Note that the data are group averages [9]. The time point of ovulation after the final dose is hardly visible in the data because the LH peak, for example, has disappeared by data averaging. Nevertheless, the simulation results agree with the reported delays of ovulation. An acute response to Cetrorelix is visible for all doses in all components (LH, FSH and E2), but the suppression of E2 in strongest in the highest dose group ($1000\mu\mathrm{g}$). Moreover, E2 values after ovulation hint to a normal luteal function, and the next cycle after treatment has normal length of 28 days.

5 Conclusion

The mathematical model developed in this paper describes the hormone profiles throughout the female menstrual cycle in correspondence with measurement values of LH, FSH, P4 and E2 for 12 individual healthy women. Unlike previous models [16, 32, 30], the new model correctly predicts the changes in the cycle following single and multiple dose administration of a GnRH agonist or antagonist at different stages in the cycle. To the best of our knowledge, this is the first mathematical model that describes such feedback mechanisms in consideration of cyclicity of the female hormonal balance.

The model applied herein for the normal cycle without GnRH analogues comprises 33 differential equations and 114 unknown parameters. Thereof 21 could be identified from the data of 12 individual women. The number of identifiable parameters increased to 52 when Nafarelin and Cetrorelix data were included. Thus we have learned more about the system by studying its reaction to external manipulations. The number of identifiable parameters might be further

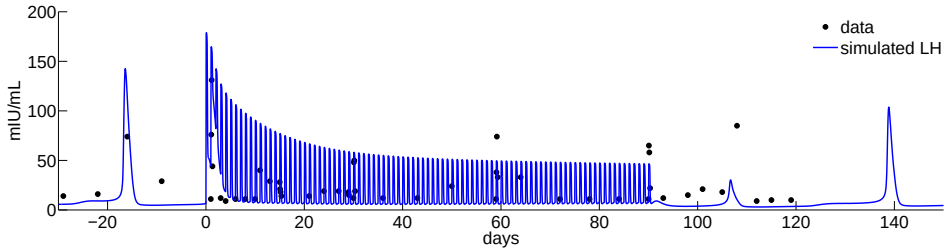

(a) LH

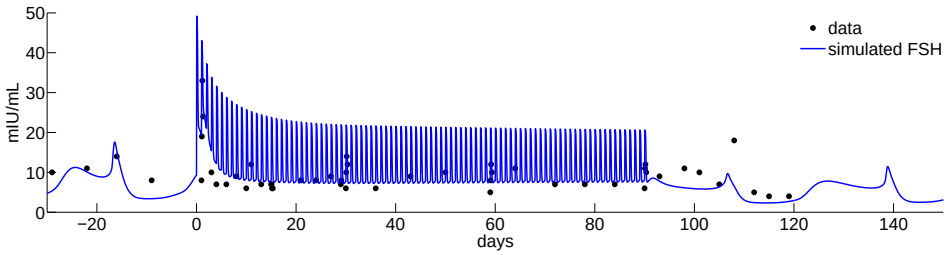

(b) FSH

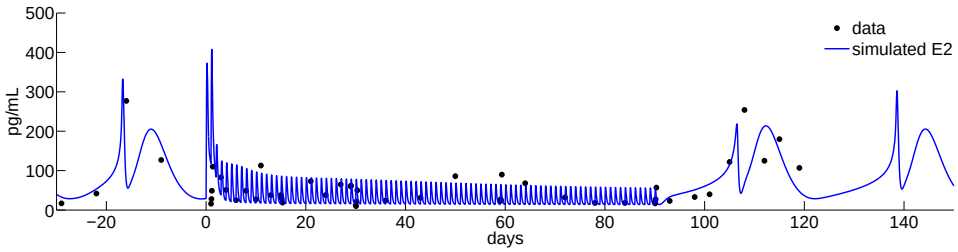

(c) E2

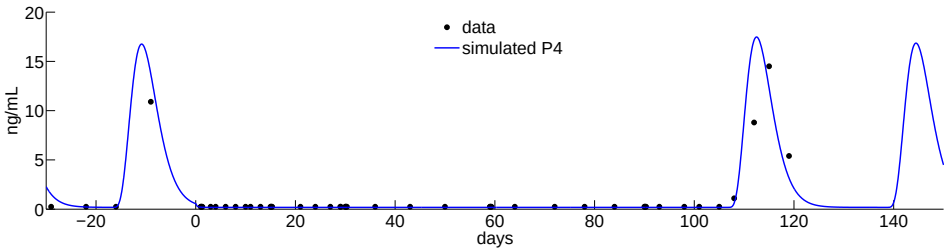

(d) P4

Figure 6: Simulation results for the daily administration of 250 μg Nafarelin on cycle days 1 to 90 (individual data from [11], also published and discussed in [26]). After an initial stimulatory phase, LH, FSH and E2 levels are suppressed but acute responses to Nafarelin are maintained, whereas P4 is suppressed constantly.

	sd/md	ID	t_0 d	t_f d	D_A μg	cl_{A_c} 1/d
Nafarelin	sd	105	5	5	100	5.48
Nafarelin	sd	208	12	12	100	9.62
Nafarelin	sd	306	22	22	100	6.00
Nafarelin	md	311	1	90	250	30
Cetrorelix	sd	Leroy1	14	14	5000	1.0
Cetrorelix	sd	Leroy2	14	14	5000	0.6
Cetrorelix	sd	Leroy3	14	14	5000	5.0
Cetrorelix	sd	Leroy4	14	14	3000	1.8
Cetrorelix	sd	Duij1	3	3	250	6.0
Cetrorelix	sd	Duij2	3	3	500	5.0
Cetrorelix	sd	Duij3	3	3	1000	5.0
Cetrorelix	md	Duij1	3	16	250	3.0
Cetrorelix	md	Duij2	3	16	500	3.0
Cetrorelix	md	Duij3	3	16	1000	3.0

Table 3: Parameters for the administration of single dose (sd) and multiple dose (md) Nafarelin or Cetrorelix. The parameter cl_A turned out to be the most sensitive and best identifiable parameter and was therefore varied between the different data sets.

reference [27]	simulation results
ovulation 15 days after Nafarelin administration, prolongation of cycle by 4.6 ± 1.7 days	ovulation 17 days (100μg) or 14 days (5μg) after Nafarelin administration
shortened cycle by 2.3 ± 1 days, statistically not significant	shortened cycle by 2 days (100μg) or 3 days (5μg)
truncated luteal phase by 4 days	truncation of luteal phase by several days, depending on the day of dosing

Table 4: A comparison between experimental observations reported in [27] (reference) and our simulation results.

increased by including more data, for example data for the administration of LH or FSH agonists or antagonists.

A key step in developing a mathematical model for the administration of GnRH analogues was the elimination of time delays and the integration of a deterministic model for the GnRH pulse pattern. The deterministic modelling turned out to be fully sufficient. In particular, in our model a nearly constant GnRH frequency, as it results for example during the multiple dose treatment with a GnRH antagonist, reduces the FSH concentration in the blood. This agrees with published observations.

The new model emphasizes the importance of time of dosing within the cycle, and it gives insight into the recovery of the cycle after the final dose. The model is robust in the sense that, after the final dose, the solution returns to the initial steady state. Beyond the results given here, a different parametrization would lead to a destabilization of the cycle, which might be an interesting topic for further investigations.

Simulation results for single and multiple dosing of Nafarelin and Cetrorelix are in good qualitative agreement with the data, but the quantitative agreement could be improved with "better" data. Ideally, the data for the dosing event would come along with measurements that were taken

	early follicular phase (ID105)	**late follicular phase (ID208)**	**luteal phase (ID306)**
LH	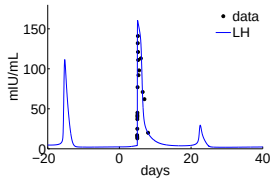	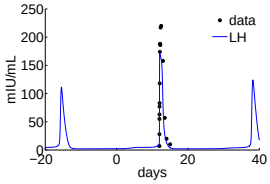	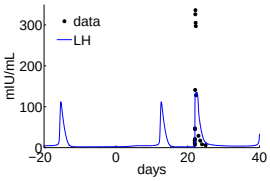
FSH	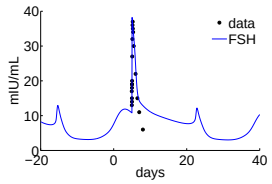	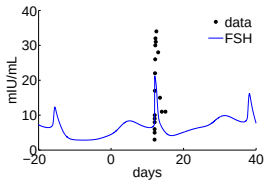	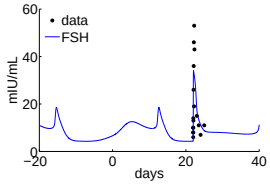
E2	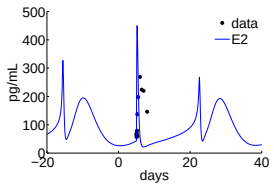	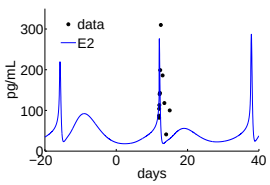	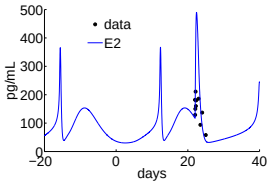
P4	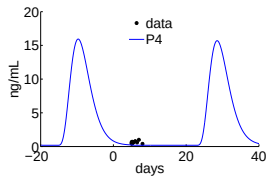	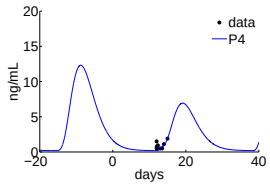	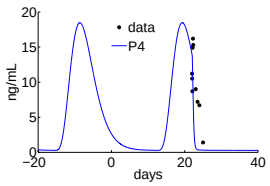
Nafarelin	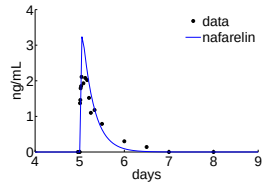	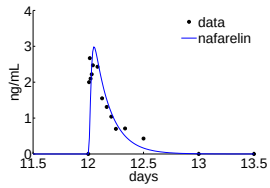	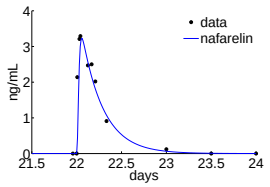

Table 5: Simulation results for the administration of 100μg Nafarelin (*single dose*) at different times in the cycle (data from [27]).

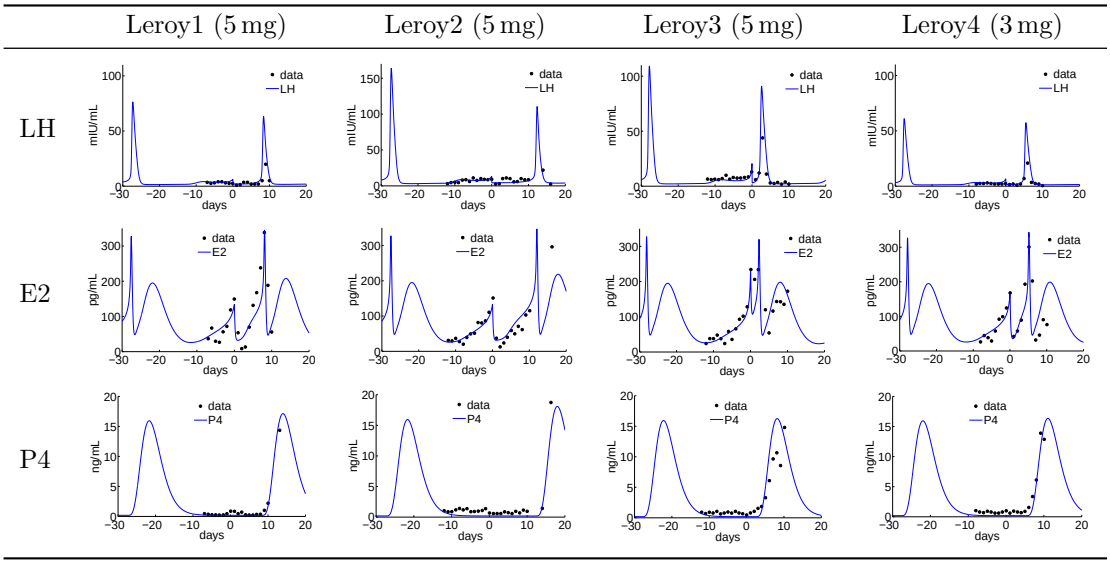

Table 6: Simulation results and data (from [23]) after the administration of 5mg (top three lines) or 3mg (bottom line) *single s.c. dose of Cetrorelix* to four representative women in the *late follicular phase*. The LH peak occurs 9, 14, 3 or 5 days after antagonist administration, depending on the individual degradation rate of Cetrorelix.

during the non-treatment cycle. This kind of data would allow for an individual parametrization of the non-treatment cycle, including individual cycle length and basal hormone levels. In this case, a better fit to individual dosing data could be obtained. However, this was not the case for the available data.

Parameter identification also gets difficult or even impossible with averaged data when averaging takes place for women with different cycle lengths and/or at different phases of the cycle as for example in [9]. The reason for this is that such data can simply not be explained by a single parametrization. Ideally, one would have individual data available, but such data are usually deleted in industry when a study is finalized and results have been published. Therefore, we hope that more companies and departments will save and provide their data in the framework of standardized data management systems.

The model could be used as starting point for further investigations. For example, in drug development one could study the influence of certain diseases on the menstrual cycle. Moreover, further testing would be required with the model to check that the parameter estimates determined from the GnRH antagonist and agonists and healthy women are viable for other therapeutic agents acting on other targets, e.g. LH and FSH. The results can then be used to explore novel targets. In order to simulate therapeutic options, our objective for the future is to not just model the idealized cycle of an "idealized woman", but to describe individual "virtual" patients by reliable models.

	Duij1 (250μg)	Duij2 (500μg)	Duij3 (1000μg)
LH	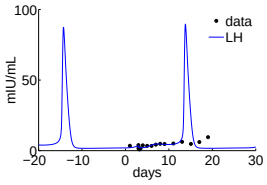	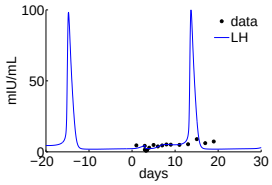	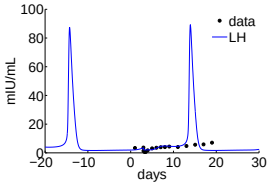
FSH	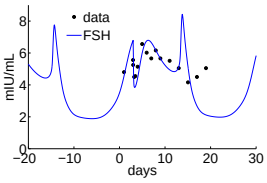	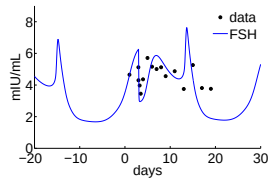	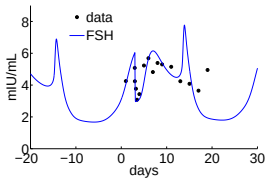
E2	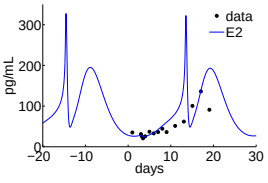	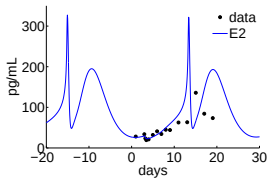	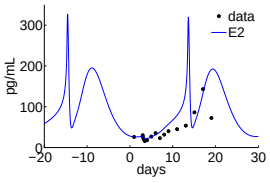
Cetrorelix	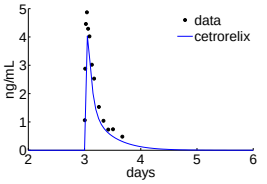	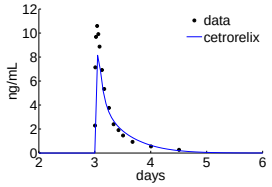	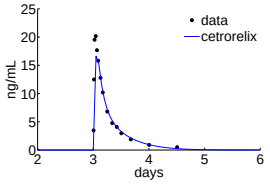

Table 7: Simulation results and data (median for $n = 12$ per group, from [9]) following *single s.c. administration of Cetrorelix* in the *early follicular phase* (cycle day 3). In all figures the time units are days. The administration did not result in an apparent delay of ovulation.

	Duij1 (250μg)	Duij2 (500μg)	Duij3 (1000μg)
LH	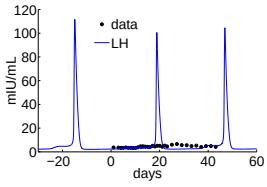	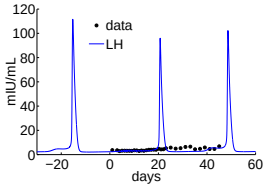	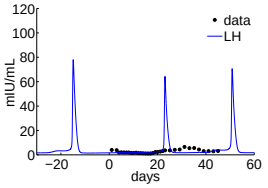
FSH	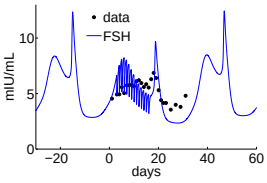	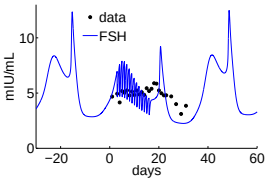	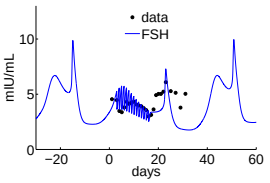
E2	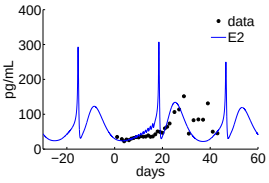	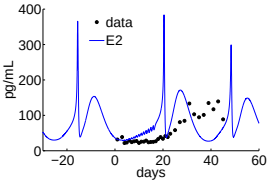	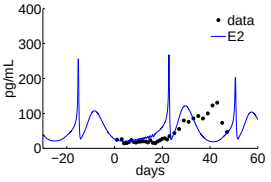
Cetrorelix	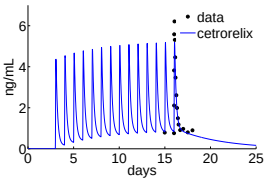	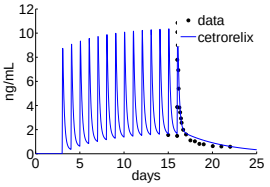	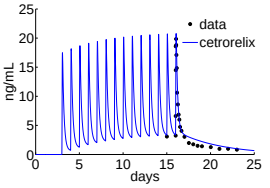

Table 8: Simulation results and data (median for $n = 12$ per group, from [9]) following *daily administration* of Cetrorelix between cycle days 3 and 16. Ovulation is delayed by 5 days (0.25mg), 10 days (5mg), or 13 days (1mg).

A Abbreviations

abbreviation	explanation
LH	luteinizing hormone
FSH	follicle stimulating hormone
E2	estradiol
P4	progesterone
IhA, IhB	inhibin A/B
IhA_{τ}	inhibin A delayed by diffusion
GnRH, G	gonadotropin releasing hormone
PrA1, PrA2	early and late primary follicle
SeF1, SeF2	early and late secondary follicle
PrF	preovulatory follicle
OvF	ovulatory follicle
Sc1, Sc2	early and late ovulatory scar
Lut1/2/3/4	development stages of corpus luteum
$\mathrm{R}_{\mathrm{LH,FSH}}$	free LH/FSH receptor
LH-R, FSH-R	LH/FSH receptor complex
$\mathrm{R}_{\mathrm{G}\,a/i}$	free active/inactive GnRH receptor
$\mathrm{G\text{-}R}_{a/i}$	active/inactive GnRH receptor complex
$\mathrm{R}_{\mathrm{LH}}^{\mathrm{foll}}$	LH receptors on follicular granulosa cells
$\mathrm{Ant}_{d/c/p}$	GnRH antagonist in dosing/central/peripheral compartment
$\mathrm{Ago}_{d/c/p}$	GnRH agonist in dosing/central/peripheral compartment
$\mathrm{Ago\text{-}R}_{a/i}$	active/inactive agonist receptor complex
Ant-R	antagonist receptor complex

B Parameter Values

Table 9: Parameter values (d=days)

No.	Symbol	value	unit	explanation	eqs.
1	$b_{\mathrm{LH}_{Syn}}$	7309.92	IU/d	basal LH synthesis rate constant	(1a)
2	$m_{\mathrm{E2}}^{\mathrm{LH}}$	7309.92	IU/d	E2 promoted LH synthesis rate constant	(1a)
3	$T_{\mathrm{E2}}^{\mathrm{LH}}$	192.2	pg/mL	threshold of E2	(1a)
4	$n_{\mathrm{E2}}^{\mathrm{LH}}$	10	–	Hill exponent	(1a)
5	$T_{\mathrm{P4}}^{\mathrm{LH}}$	2.371	ng/mL	threshold of P4	(1a)
6	$n_{\mathrm{P4}}^{\mathrm{LH}}$	1	–	Hill exponent	(1a)
7	$b_{\mathrm{LH}_{Rel}}$	0.00476	1/d	basal LH release rate constant	(1b)
8	$m_{\mathrm{G\text{-}R}}^{\mathrm{LH}}$	0.1904	1/d	influence of GnRH receptor complex on LH release	(1b)
9	$T_{\mathrm{G\text{-}R}}^{\mathrm{LH}}$	0.0003	nmol/l	threshold of GnRH on LH release rate	(1b)
10	$n_{\mathrm{G\text{-}R}}^{\mathrm{LH}}$	5	–	Hill exponent	(1b)
11	V_{blood}	6.589	L	blood volume	(2),(7)

Continued on next page...

Table 9 – *continued from previous page*

No.	Symbol	value	unit	explanation	eqs.
12	k_{on}^{LH}	2.143	L/(d·IU)	binding rate of LH to its receptor	(2)–(4)
13	cl_{LH}	74.851	1/d	clearance rate of LH from the blood	(2)
14	k_{recy}^{LH}	68.949	1/d	formation rate of free LH receptors	(3),(5)
15	k_{des}^{LH}	183.36	1/d	desensitization rate of LH receptor complex	(4),(5)
16	$T_{\mathrm{freq}}^{\mathrm{FSH}}$	0.8	1/d	threshold of GnRH frequency	(6a)
17	$n_{\mathrm{freq}}^{\mathrm{FSH}}$	5	–	Hill exponent	(6a)
18	$m_{\mathrm{Ih}}^{\mathrm{FSH}}$	2.213e+4	IU/d	basal FSH synthesis rate constant	(6a)
19	T_{IhA}	95.81	IU/mL	threshold of Inhibin A in FSH synthesis	(6a)
20	T_{IhB}	70	pg/mL	threshold of Inhibin B in FSH synthesis	(6a)
21	n_{IhA}	5	–	Hill exponent	(6a)
22	n_{IhB}	2	–	Hill exponent	(6a)
23	$b_{\mathrm{FSH}_{Rel}}$	0.05699	1/d	basal FSH release rate constant	(6b)
24	$m_{\mathrm{G\text{-}R}}^{\mathrm{FSH}}$	0.272	1/d	stimulation of FSH release by GnRH receptor complex	(6b)
25	$T_{\mathrm{G\text{-}R}}^{\mathrm{FSH}}$	0.0003	nmol/l	threshold of GnRH on FSH release rate	(6b)
26	$n_{\mathrm{G\text{-}R}}^{\mathrm{FSH}}$	2	–	Hill exponent for FSH release	(6b)
27	k_{on}^{FSH}	3.529	L/(d·IU)	binding rate of FSH to its receptor	(7)–(9)
28	cl_{FSH}	144.25	1/d	clearance rate of FSH from the blood	(7)
29	k_{recy}^{FSH}	61.029	1/d	formation rate of free FSH receptors	(8),(10)
30	k_{des}^{FSH}	138.3	1/d	desensitization rate of FSH receptor complex	(9),(10)
31	$T_{\mathrm{FSH}}^{\mathrm{R_{LH}}}$	0.5	$[\mathrm{R}_{\mathrm{LH}}^{\mathrm{foll}}]$	threshold of FSH-R to stimulate LH receptors on granulosa cells	(11)
32	$n_{\mathrm{FSH}}^{\mathrm{R_{LH}}}$	5	–	Hill exponent	(11)
33	$T_{\mathrm{P4}}^{\mathrm{R_{LH}}}$	1.235	ng/mL	threshold of P4 for clearance of LH receptors on granulosa cells	(11)
34	$n_{\mathrm{P4}}^{\mathrm{R_{LH}}}$	5	–	Hill exponent	(11)
35	$m_{\mathrm{FSH}}^{\mathrm{R_{LH}}}$	0.219	$[\mathrm{R}_{\mathrm{LH}}^{\mathrm{foll}}]$/d	synthesis rate constant of LH receptors on granulosa cells	(11)
36	$m_{\mathrm{P4}}^{\mathrm{R_{LH}}}$	1.343	1/d	$\mathrm{R}_{\mathrm{LH}}^{\mathrm{foll}}$ clearance rate constant	(11)
37	$m_{\mathrm{OvF}}^{\mathrm{Sc1}}$	1.208	1/d	growth rate of Sc1 stimulated by OvF	(18)
38	$m_{\mathrm{PrF}}^{\mathrm{OvF}}$	7.984	1/d	growth rate of OvF	(17)
39	$k_{\mathrm{SeF1}}^{\mathrm{SeF1}}$	0.122	l/(d·nmol)	self growth rate of SeF1	(14)

Continued on next page...

Table 9 – *continued from previous page*

No.	Symbol	value	unit	explanation	eqs.
40	$k_{\mathrm{SeF1}}^{\mathrm{SeF2}}$	122.06	1/d	transition rate constant from SeF1 to SeF2	(14),(15)
41	$k_{\mathrm{SeF2}}^{\mathrm{SeF2}}$	12.206	1/d	self growth rate of SeF2	(15)
42	$k_{\mathrm{SeF2}}^{\mathrm{PrF}}$	332.75	1/d	transition rate constant from SeF2 to PrF	(16)
43	cl_{PrF}	122.06	1/d	elimination rate constant of PrF	(16)
44	cl_{OvF}	12.206	1/d	elimination rate constant of OvF	(17)
45	$k_{\mathrm{Sc1}}^{\mathrm{Sc2}}$	1.221	1/d	transition rate constant from Sc1 to Sc2	(18),(19)
46	$k_{\mathrm{Sc2}}^{\mathrm{Lut1}}$	0.959	1/d	transition rate constant from Sc2 to Lut1	(19),(20)
47	$k_{\mathrm{Lut1}}^{\mathrm{Lut2}}$	0.925	1/d	transition rate constant from Lut1 to Lut2	(20),(21)
48	$k_{\mathrm{Lut2}}^{\mathrm{Lut3}}$	0.7567	1/d	transition rate constant from Lut2 to Lut3	(21),(22)
49	$k_{\mathrm{Lut3}}^{\mathrm{Lut4}}$	0.61	1/d	transition rate constant from Lut3 to Lut4	(22),(23)
50	cl_{Lut4}	0.543	1/d	clearance rate constant of Lut4	(23)
51	$n_{\mathrm{SeF1}}^{\mathrm{SeF2}}$	5	–	Hill exponent	(14),(15)
52	n_{SeF2}	2	–	Hill exponent	(15)
53	$n_{\mathrm{PrF}}^{\mathrm{OvF}}$	6.308	–	Hill exponent	(16),(17)
54	$n_{\mathrm{PrA2}}^{\mathrm{SeF1}}$	3.689	–	Hill exponent	(13),(14)
55	$n_{\mathrm{FSH}}^{\mathrm{PrA1}}$	5	–	Hill exponent	(12)
56	$T_{\mathrm{FSH}}^{\mathrm{PrA1}}$	0.608	nmol/L	threshold of FSH receptor complex for stimulation of PrA1	(12)
57	$m_{\mathrm{FSH}}^{\mathrm{PrA1}}$	3.662	[PrA1]/d	growth rate of PrA1	(12)
58	$k_{\mathrm{PrA1}}^{\mathrm{PrA2}}$	1.221	L/(d·nmol)	transition rate constant from PrA1 to PrA2	(12),(13)
59	$k_{\mathrm{PrA2}}^{\mathrm{SeF1}}$	4.882	1/d	transition rate constant from PrA2 to SeF1	(13),(14)
60	$SF_{\mathrm{LH\text{-}R}}$	2.726	nmol/L	scaling of LH receptor complex	(14)-(17)
61	$T_{\mathrm{PrF}}^{\mathrm{OvF}}$	3	[PrF]	threshold of PrF for OvF formation	(17)
62	$n_{\mathrm{PrF}}^{\mathrm{OvF}}$	10	–	Hill exponent	(17)
63	SeF_{max}	10	[SeF1]	maximum size of SeF1 and SeF2	(14),(15)
64	$T_{\mathrm{OvF}}^{\mathrm{Sc1}}$	0.02	[OvF]	threshold of OvF to form Sc1	(18)
65	$n_{\mathrm{OvF}}^{\mathrm{Sc1}}$	10	–	Hill exponent	(18)

Continued on next page...

Table 9 – *continued from previous page*

No.	Symbol	value	unit	explanation	eqs.
66	$m^{\mathrm{Lut}}_{\mathrm{G\text{-}R}}$	20	[Lut1]	effect of G-R to stimulate luteal development	(20)–(23)
67	$T^{\mathrm{Lut}}_{\mathrm{G\text{-}R}}$	0.0008	[G-R]	threshold of G-R to stimulate luteal development	(20)–(23)
68	$n^{\mathrm{Lut}}_{\mathrm{G\text{-}R}}$	5.395	[G-R]	Hill exponent	(20)–(23)
69	b_{E2}	51.558	pg/(mL·d)	basal E2 production	(24)
70	$k^{\mathrm{E2}}_{\mathrm{PrA2}}$	2.095	g/(mol·[PrA2])	production of E2 by PrA2	(24)
71	$k^{\mathrm{E2}}_{\mathrm{SeF1}}$	309343.1	pg/(mL·[SeF1]·d)	production of E2 by SeF1	(24)
72	$k^{\mathrm{E2}}_{\mathrm{SeF2}}$	6960.53	pg/(mL·[SeF2]·d)	production of E2 by SeF2	(24)
73	$k^{\mathrm{E2}}_{\mathrm{PrF}}$	161848.9	pg/(mL·[PrF]·d)	production of E2 by PrF	(24)
74	$k^{\mathrm{E2}}_{\mathrm{Lut1}}$	1713.71	pg/(mL·[Lut1]·d)	production of E2 by Lut1	(24)
75	$k^{\mathrm{E2}}_{\mathrm{Lut4}}$	8675.14	pg/(mL·[Lut4]·d)	production of E2 by Lut4	(24)
76	cl_{E2}	5.235	1/d	E2 clearance rate constant	(24)
77	b_{P4}	0.943	ng/(mL·d)	basal P4 production	(25)
78	$k^{\mathrm{P4}}_{\mathrm{Lut4}}$	761.64	ng/(mL·[Lut4]·d)	production of P4 by Lut4	(25)
79	cl_{P4}	5.13	1/d	P4 clearance rate constant	(25)
80	b_{IhA}	1.445	IU/mL/d	basal IhA production	(26)
81	$k^{\mathrm{IhA}}_{\mathrm{PrF}}$	2.285	IU/mL/([PrF]·d)	production of IhA by PrF	(26)
82	$k^{\mathrm{IhA}}_{\mathrm{Sc1}}$	60	pg/mL/([Sc1]·d)	production of IhA by Sc1	(26)
83	$k^{\mathrm{IhA}}_{\mathrm{Lut1}}$	180	pg/mL/([Lut1]·d)	production of IhA by Lut1	(26)
84	$k^{\mathrm{IhA}}_{\mathrm{Lut2}}$	28.211	IU/mL/([Lut2]·d)	production of IhA by Lut2	(26)
85	$k^{\mathrm{IhA}}_{\mathrm{Lut3}}$	216.85	IU/mL/([Lut3]·d)	production of IhA by Lut3	(26)
86	$k^{\mathrm{IhA}}_{\mathrm{Lut4}}$	114.25	IU/mL/([Lut4]·d)	production of IhA by Lut4	(26)
87	cl_{IhA}	4.287	1/d	Inh A clearance rate constant	(26),(28)
88	cl_{IhA_τ}	0.199	1/d	clearance of Inhibin A in delayed compartment	(28)
89	b_{IhB}	89.493	pg/mL/d	basal IhB production	(27)
90	$k^{\mathrm{IhB}}_{\mathrm{PrA2}}$	447.47	pg/mL/([PrA2]·d)	production of IhB by PrA2	(27)
91	$k^{\mathrm{IhB}}_{\mathrm{Sc2}}$	134240.2	pg/mL/([SeF1]·d)	production of IhB by Sc2	(27)
92	cl_{IhB}	172.45	1/d	Inh B clearance rate constant	(27)
93	k^{freq}	1	1/d	mean GnRH pulse frequency	(29a)
94	$T^{\mathrm{freq}}_{\mathrm{P4}}$	1.2	ng/mL	threshold of P4 for inhibition of GnRH frequency	(29a)
95	$n^{\mathrm{freq}}_{\mathrm{P4}}$	2	–	Hill exponent	(29a)

Continued on next page...

Table 9 – *continued from previous page*

No.	Symbol	value	unit	explanation	eqs.
96	$m_{\mathrm{E2}}^{\mathrm{freq}}$	1	–	stimulation of frequency by E2	(29a)
97	$T_{\mathrm{E2}}^{\mathrm{freq}}$	220	pg/mL	threshold of E2 for stimulation of GnRH frequency	(29a)
98	$n_{\mathrm{E2}}^{\mathrm{freq}}$	10	–	Hill exponent	(29a)
99	k^{mass}	0.0895	nmol	amount of GnRH released by one pulse at high E2 concentration	(29b)
100	$T_{\mathrm{E2}}^{\mathrm{mass,1}}$	220	pg/mL	threshold of E2 for stimulation of GnRH mass	(29b)
101	$n_{\mathrm{E2}}^{\mathrm{mass,1}}$	2	–	Hill exponent	(29b)
102	$T_{\mathrm{E2}}^{\mathrm{mass,2}}$	9.6	pg/mL	threshold of E2 for inhibition of GnRH mass	(29b)
103	$n_{\mathrm{E2}}^{\mathrm{mass,2}}$	1	–	Hill exponent	(29b)
104	k_{degr}^{G}	0.447	1/d	degradation rate of GnRH	(29)
105	k_{on}^{G}	322.18	L/(d·nmol)	binding rate of GnRH to its receptor	(29), (30),(32)
106	k_{off}^{G}	644.35	1/d	breakup rate of GnRH-receptor complex	(29), (30),(32)
107	$k_{degr}^{\mathrm{G\text{-}R}_i}$	0.00895	1/d	degradation rate of inactive receptor complex	(33)
108	$k_{diss}^{\mathrm{G\text{-}R}_i}$	32.218	1/d	dissociation rate of inactive receptor complex	(31),(33)
109	$k_{inter}^{\mathrm{R_G}}$	3.222	1/d	rate of receptor inactivation	(30),(31)
110	$k_{recy}^{\mathrm{R_G}}$	32.218	1/d	rate of receptor activation	(30),(31)
111	$k_{degr}^{\mathrm{R_G}}$	0.0895	1/d	degradation rate of inactive receptors	(31)
112	$k_{inact}^{\mathrm{G\text{-}R}}$	32.218	1/d	rate of receptor complex inactivation	(32),(33)
113	$k_{act}^{\mathrm{G\text{-}R}}$	3.222	1/d	rate of receptor complex activation	(32),(33)
114	$k_{syn}^{\mathrm{R_G}}$	8.949e-5	nmol/(L·d)	synthesis rate of inactive receptors	(31)

C Initial Values

Table 10: Initial values

No.	component	value	unit
1	$\mathrm{LH}_{\mathrm{pit}}$	3.572e+05	IU
2	LH_{blood}	6.619	IU/L
3	R_{LH}	7.304	nmol/L
4	LH-R	0.565	nmol/L
5	$\mathrm{R}_{\mathrm{LH},des}$	1.5032	nmol/L

Continued on next page...

Table 10 – *continued from previous page*

No.	component	value	unit
6	FSH_{pit}	3.737e+4	IU
7	FSH_{blood}	5.762	IU/L
8	R_{FSH}	5.741	nmol/L
9	FSH-R	0.844	nmol/L
10	$R_{FSH,des}$	1.915	nmol/L
11	R_{LH}^{foll}	1.597	–
12	PrA1	2.943	[Foll]
13	PrA2	38.995	[Foll]
14	SeF1	3.652	[Foll]
15	SeF2	2.478e-3	[Foll]
16	PrF	0.8755	[Foll]
17	OvF	1.822e-10	[Foll]
18	Sc1	1.087e-13	[Foll]
19	Sc2	2.572e-10	[Foll]
20	Lut1	7.055e-9	[Foll]
21	Lut2	4.066e-7	[Foll]
22	Lut3	1.557e-5	[Foll]
23	Lut4	1.852e-4	[Foll]
24	E2	60.454	pg/mL
25	P4	0.2142	ng/mL
26	IhA	0	IU/mL
27	IhB	0	pg/mL
28	IhA_{τ}	30.42	IU/mL
29	G	3.1806e-2	nmol/L
30	$R_{G,a}$	8.9738e-3	nmol/L
31	$R_{G,i}$	1.0214e-3	nmol/L
32	G-R_a	1.3650e-4	nmol/L
33	G-R_i	1.2408e-4	nmol/L
34	Ago_d	0	μg
35	Ago_c	0	μg/L=ng/mL
36	Ago_p	0	μg/L=ng/mL
37	Ago-R_a	0	nmol/L
38	Ago-R_i	0	nmol/L
39	Ant-R	0	nmol/L
40	Ant_c	0	μg/L=ng/mL
41	Ant_d	0	μg
42	Ant_p	0	μg/L=ng/mL

The presented model equations are consistent with respect to physical units. Since we wanted the units of the output curves for measured quantities to agree with the (inconsistent) units of the corresponding measurement values, we introduced correction factors SF_{Ago} and SF_{Ant} in the model equations to account for the conversion of units. These factors were computed from the molar weights,

$$M_{\mathrm{Naf}} = 1322.49\mathrm{g/mol}, \qquad M_{\mathrm{Cet}} = 1431.06\mathrm{g/mol}.$$

Since Nafarelin is measured in ng/mL (1 ng/mL $= 10^{-6}\,$g/L $\equiv \frac{10^{-6}\,\mathrm{g/L}}{1322.49\,\mathrm{g/mol}} = 0.7561$ nmol/L), we decided for nmol/L as unit for the unknown quantities (receptors, receptor complexes). The conversion of units for Cetrorelix conforms to 1 ng/mL$\equiv \frac{10^{-6}\,\mathrm{g/L}}{1431.06\,\mathrm{g/mol}} = 0.6988$ nmol/L. Thus,

$$SF_{\mathrm{Ago}} = 0.7561\,\mathrm{ng/pmol}, \quad SF_{\mathrm{Ant}} = 0.6988\,\mathrm{ng/pmol}.$$

The physical units of all system components are listed in Tab. 10.

References

[1] NLSCON, Nonlinear Least Squares with nonlinear equality CONstraints. `http://www.zib.de/en/numerik/software/codelib/nonlin.html`.

[2] J. J. Blum, M. C. Reed, J. A. Janovick, and P. M. Conn. A mathematical model quantifying GnRH-induced LH secretion from gonadotropes. *Am. J. Physiol. Endocrinol. Metab.*, 278:E263–E272, 2000.

[3] D.W.A. Bourne. *Mathematical Modeling of Pharmacokinetic Data.* Taylor and Francis, Inc., 1995.

[4] N. Chabbert-Buffet and P. Bouchard. The normal human menstrual cycle. *Rev. Endocr. Metab. Disord.*, 3:173–183, 2002.

[5] P. Deuflhard. *Newton Methods for Nonlinear Problems: Affine Invariance and Adaptive Algorithms.* Number 35 in Springer Series in Computational Mathematics. Springer Verlag, Berlin, 2004.

[6] P. Deuflhard and A. Hohmann. *Numerical Analysis in Modern Scientific Computing - An Introduction.* Texts in Applied Mathematics. Springer, New York, 2nd edition, 2003.

[7] P. Deuflhard and U. Nowak. Efficient numerical simulation and identification of large chemical reaction systems. *Ber. Bunsenges. Phys. Chem*, 90:940–946, 1986.

[8] T. Dierkes, M. Wade, U. Nowak, and S. Röblitz. BioPARKIN - Biology-related parameter identification in large kinetic networks. ZIB-Report 11-15, Zuse Institute Berlin (ZIB), 2011. `http://vs24.kobv.de/opus4-zib/frontdoor/index/index/docId/1270`.

[9] I.J.M. Duijkers, C. Klipping, W.N.P. Willemsen, D. Krone, E. Schneider, G. Niebch, and R. Hermann. Single and multiple dose pharmacokinetics and pharmacodynamics of the gonadotropin-releasing hormone antagonist Cetrorelix in healthy female volunteers. *Hum. Reprod.*, 13(9):2392–2398, 1998.

[10] J. B. Engel and A. V. Schally. Drug insight: clinical use of agonists and antagonosts of luteinizing-hormone-releasing hormone. *Nature Clinical Practice*, 3(2):157–167, 2007.

[11] R.J. Jaffe et al. Inhibition of ovulation by Nafarelin in normal women and women with endometriosis: nasal formulation. ICM Study 1010, Syntex Research, Palo Alto, California, 1986.

[12] M. B. Garnick. History of GnRH antagonists in the management of hormonally responsive disorders a historical overview. Abstract for the 6th International Symposium on GnRH analogues in cancer and human reproduction, Geneva, Switzerland, February 2001. `http://www.kenes.com/gnrh2001/Abstracts/0112aGarnick.htm`.

[13] F. S. Greenspan and G. J. Strewler (ed.). *Basic Clin. Endocrinol.* 5th edition. Appleton & Lange, 1997.

[14] N. P. Groome, P. J. Illingworth, M. O'Brien, R. Pai, F. E. Rodger, J. P. Mather, and A. S. McNeilly. Measurement of dimeric inhibin B throughout the human menstrual cycle. *J. Clin. Endocrinol. Metab.*, 81(4):1401–1405, 1996.

[15] J. E. Hall. Neuroendocrine control of the menstrual cycle. In R. L. Barbieri Strauss, editor, *Yen and Jaffe's Reproductive Endocrinology: Physiology, Pathophysiology, and Clinical Management*, chapter 7, pages 139–154. Saunders Elsevier, 6 edition, 2009.

[16] L. A. Harris. *Differential Equation Models for the Hormonal Regulation of the Menstrual Cycle.* PhD thesis, North Carolina State University, 2001.

[17] L. Harris Clark, P. M. Schlosser, and J. F. Selgrade. Multiple stable periodic solutions in a model for hormonal control of the menstrual cycle. *Bull. Math. Biol.*, 65:157–173, 2003.

[18] F. Hayes, J. E. Hall, P. A. Boepple, and Jr. W. F. Crowly. Differential control of gonadotropin secretion in the human: Endocrine role of inhibin. *J. Clin. Endocrinol. Metab.*, 83:1835–1841, 1998.

[19] K. Heinze, R. W. Keener, and A. R. Midgley Jr. A mathematical model of luteinizing hormone release from ovine pituitary cells in perifusion. *Am. J. Physiol. Endocrinol. Metab.*, 275:E1061–E1071, 1998.

[20] P.R. Jadhav, H. Agersø, C. Tornoe, and J.V.S. Gobburu. Semi-mechanistic pharmacodynamic modeling for degarelix, a novel gonadotropin releasing hormone (GnRH) blocker. *J. Pharmacokinet.Pharmacodyn.*, 33(5):609–634, 2006.

[21] C. Keck, J. Neulen, H. M. Behre, and M. Breckwoldt. *Endokrinologie, Reproduktionsmedizin, Andrologie.* 2nd edition. Georg Thieme Verlag, 2002.

[22] B.-F. Krippendorff, K. Kuester, Ch. Kloft, and W. Huisinga. Nonlinear pharmacokinetics of therapeutic proteins resulting from receptor mediated endocytosis. *J. Pharmacokinet. Pharmacodyn.*, 36:239–260, 2009. 10.1007/s10928-009-9120-1.

[23] I. Leroy, M.F. d'Acremont, S. Brailly-Tabard, R. Frydman, J. de Mouzon, and P. Bouchard. A single injection of a gonadotropin-releasing hormone (GnRH) antagonist (Cetrorelix) postpones the luteinizing hormone (LH) surge: further evidence for the role of GnRH during the LH surge. *Fertil. Steril.*, 62(3):461–467, 1994.

[24] R.I. McLachlan, N.L. Cohen, K.D. Dahl, W.J. Bremner, and M.R. Soules. Serum inhibin levels during the periovulatory interval in normal women: Relationships with sex steroid and gonadotrophin levels. *Clin. Endocrinol.*, 32:39–48, 1990.

[25] Merck. The Merck manuals online medical library, 2010.

[26] S.E. Monroe, Z. Blumenfeld, J.L. Andreyko, E. Schriock, M.R. Henzl, and R.B. Jaffe. Dose-dependent inhibition of pituitary-ovarian function during administration of a gonadotropin-releasing hormone agonistic analog (Nafarelin). *J. Clin. Endocrinol. Metab.*, 63(6):1334–1341, 1986.

[27] S.E. Monroe, M.R. Henzl, M.C. Martin, E. Schriock, V. Lewis, C. Nerenberg, and R.B. Jaffe. Ablation of folliculogenesis in women by a single dose of gonadotropin-releasing hormone agonist: significance of time in cycle. *Fertil. Steril.*, 43(8):361–368, 1985.

[28] N.V. Nagaraja, B. Pechstein, K. Erb, C. Klipping, R. Hermann, M. Locher, and H. Derendorf. Pharamacokinetik/pharamcodynamic modeling of luteinizing hormone (LH) suppression and LH surge delay by Cetrorelix after single and multiple doses in healthy premenopausal women. *J. Clin. Pharmacol.*, 43:243–251, 2003.

[29] U. Nowak and P. Deuflhard. Numerical identification of selected rate constants in large chemical reaction systems. *Appl. Numer. Math.*, 1(1):59–75, 1985.

[30] R. D. Pasteur. *A Multiple-Inhibin Model of the Human Menstrual Cycle.* PhD thesis, North Carolina State University, 2008.

[31] I. Reinecke. *Mathematical modeling and simulation of the female menstrual cycle.* PhD thesis, Freie Universität Berlin, 2009.

[32] I. Reinecke and P. Deuflhard. A complex mathematical model of the human menstrual cycle. *J. Theor. Biol.*, 247:303–330, 2007.

[33] P. M. Schlosser and J. F. Selgrade. A model of gonadotropin regulation during the menstrual cycle in women: Qualitative features. *Enviro. Health Perspect.*, 108(5):873–881, 2000.

[34] A. Sehested, A. Juul, A.M. Andersson, J.H. Petersen, T.K. Jensen, J. Müller, and N.E. Skakkebaek. Serum inhibin A and inhibin B in healthey prepubertal, pubertal, and adolescent girls and adult women: Relation to age, stage of puberty, menstrual cycle, follicle-stimulating hormone, luteinizing hormone, and estradiol levels. *J. Clin. Endocrinol. Metab.*, 85(4):1634–1640, 2000.

[35] J.F. Selgrade. Modeling hormonal control of the menstrual cycle. *Comments Theor. Biol.*, 6(1):79–101, 2001.

[36] J.F. Selgrade and P.M. Schlosser. A model for the production of ovarian hormones during the menstrual cycle. *Fields Inst. Commun.*, 21:429–446, 1999.

[37] R.S. Swerdloff, H.S. Jacobs, and W.D. Odell. Synergistic role of progestogens in estrogen induction of LH and FSH surge. *Endocrinology*, 90(6):1529–1536, 1972.

[38] C.W. Tornœ, H. Agersø, T. Senderovitz, H.A. Nielsen, H. Madsen, M.O. Karlsson, and E.N. Jonsson. Population pharmacokinetic/pharmacodynamic (PK/PD) modelling of the hypothalamic-pituitary-gonadal axis following treatment with gnrh analogues. *Br. J. Clin. Pharmacol.*, 63(6):648–664, 2006.

[39] A. J. Zeleznik and C. R. Pohl. Control of follicular development, corpus luteum function, the maternal recognition of pregnancy, and the neuroendocrine regulation of the menstrual cycle in higher primates. In J. D. Neill, editor, *Knobil and Neill's Physiology of Reproduction*, volume 2, chapter 45, pages 2449–2510. Elsevier, 3 edition, 2006.